VII FORMATION FROM SOLUTION

VII.1 Principles

The first method used for the formation of fibers utilized polymer solutions. The first patent for fiber formation was for wet formation and was issued in 1885.[1] Historically, the second was dry formation, introduced around 1904.[2] Both of the methods using polymer solutions continue to be used today, with a large volume of fibers being manufactured commercially using the solution techniques. Moreover, the newest *high performance* fibers are produced mainly in wet processes. In the future, wet processes may be even more important, though formation from the melt is the choice technique today.

In essence, there is only one significant difference between formation from solution and from melt: the presence of a solvent in the polymer stream. Nevertheless, the solvent has a dramatic influence on many of the "unit" processes of fiber formation.[3–9] The crystallization rate increases with increasing concentration of the solution, even at the same degree of undercooling.[6–9] The process of crystallization from solution takes a much different course than the crystallization from melt. There is no maximum in the rate of crystallization from solution *versus* temperature, or the maximum is shifted toward much higher degrees of undercooling. Strain, or mechanical stretching of dissolved polymer molecules, initiates crystallization as it does in the melts. Relaxation and retardation times of polymers in solution are substantially shorter and this has great significance for the processing. The polymer habits in crystallization from solution show why it is practically impossible to obtain a low degree of crystallinity in spun fibers, unless the particular polymer crystallizes slowly and poorly by its nature.

Another factor needs to be stressed: we shall discuss only a system consisting of a polymer and a given solvent. Change of solvent changes everything else, at least to some degree. System properties depend on the both components alike, on polymer type and on solvent type.

The viscosity of solutions is lower than the viscosity of melts. The viscosity dependence on the molecular mass is of the same significance, as is the influence of abnormalities of any kind in the polymer architecture. Shear affects solutions in the same way, but the effects are shorter lasting due to the short relaxation times. Similar differences are in molecule entanglements and their persistence. The effective temperature of crystallization is equally important as in formation from the melt. All that concerns neck drawing retains its importance and its influence has similar power.

The concentration of a polymer solution changes during processing, and this must be respected in the material balance. The equation describing strain must include the local concentration, the volume of polymer solution decreases with increasing distance from the spinnerette, $Q_{n-1} > Q_n$ and thus $Q_n/Q_{n-1} < 1$

$$\delta = \frac{v_n}{v_{n-1}} = \frac{Q_n d_{n-1}^2}{Q_{n-1} d_n^2} \tag{VII.1}$$

In effect, then, the true extension ratio in formation from solution is always smaller than it would appear just from the measurement of filament diameter.

Very few processes of fiber formation from solution permit us to obtain the spun fibers completely free of solvents. The residual solvents swell the fiber structure to some extent If the crystallization is not complete, then the residual solvent may cause it to proceed further as a kind of secondary crystallization. In practice, however, low crystallinity in fibers formed from solution is extremely rare. A low degree of crystallinity in spun fibers may be obtained if the polymer crystallizes badly. For these reasons, conventional extensive neck drawing may be difficult. If there is a need for a high degree of neck drawing, more drastic drawing conditions must applied, for example several stages of high temperature to allow "recrystallization" through a chain translation.

The above considerations indicate that the selection of a proper solvent presents a task as difficult as it is important. Unfortunately, there are no ready-made recipes to help. At this point one may suggest only a certain number of general criteria which a solvent must satisfy.[2] As such criteria one may quote:

- ability to form concentrated solutions
- convenient boiling point
- good heat stability
- ease of recovery
- low heat of evaporation
- physiological inactivity
- chemical inertness to the dissolved polymer, e.g. no cross linking.

The last point, naturally, does not concern processes which are built on a chemical modification of the polymer to achieve solubility, like in the cases of processing cellulose. When such a reactivity is needed, this becomes an additional strict requirement. For commercial operations, the price of the solvent is a matter of great significance. Conventional formation of common fibers from solution is thus far satisfied by only a few solvents: acetone, carbon disulfide, dimethylformamide, sodium thiocyanate in water, and tetrahydrofuran. The "ideal" solvent would have the ability to form relatively highly concentrated solutions of high molecular mass polymers at relatively low viscosities. Although there is a contradiction in these criteria, there is a matter of extent. Some solvents perform better than others, are closer to the "ideal". Safety of operations benefits when the solvent does not have too low an electrical conductivity. These criteria are essential from the point of view of the ease of processing, of fiber quality, and process economy, as well as for the safety of the operating crew and equipment. Formation from solution present additional hazards, but modern technologies are able to cope with the hazards easily.

If one considers the technological aspects, the formation of fibers from solution differs from the formation from the melt by one more important point. In formation from melt the main parameters of fiber solidification are filament temperature and diameter profiles, with the other process variables playing a somewhat auxiliary role. If the velocity of take-up and rate of extrusion are constant, then the rheological properties govern the attenuation of the filament diameter. The diameter profile is a result of the temperature profile and its influence on the rheological properties of the polymer. Constant cooling conditions, with the other parameters constant, determine the actual temperature profile. And in this way the magic circle is closed. In fiber formation from solution, an additional member has to be added to this ring - diffusion. The removal of solvent, in a dry process or wet, is governed by the rate of diffusion and on the filament diameter. The diffusivity depends on the temperature and polymer concentration.[10-13] For those processes where besides diffusion osmosis also appears, the question becomes more complicated.[14] When the solvent removal from the fiber is rapid in relation to the velocity of the solvent diffusion from the fiber core towards its surface, a sheath of solid or almost solid polymer may be formed around a relatively low concentrated solution core. When this takes place, further solvent removal is additionally complicated by the necessity of solvent osmosis through a layer of solid, or almost solid, polymer. Such a course of events is also behind the mechanism which causes the fibers to have nonround cross sections. The almost solid sheath is usually formed in the beginning of solidification when the volume and diameter of the fiber are still large. The subsequent loss of solvent through the sheath is governed by osmosis and can cause a decrease of volume of about the same size as the solid sheath. The vacuum created inside causes the oversized skin to collapse and form wrinkles on the surface, or forms cavities in the fiber core, or both. In such a way microvoids or microcracks dispersed across the whole filament are formed.[15-17] The degree of the process dependence on osmosis and the degree of collapse of the cylindrical fiber are strongly interrelated.

VII.2 Diffusion in Fiber Formation

Several papers describing diffusion in fiber formation from solution have been published,[12,18-20] they pertain mainly to the wet process. The important approaches are quoted here.

Griffin and Coghanowr[21] have considered diffusion of copper ions into fibers beginning with the following equation of diffusion:

$$\frac{\partial c_t}{\partial t} = D\frac{\partial^2 c_t}{\partial r^2} + \frac{1}{r} \cdot \frac{\partial c_t}{\partial r} \qquad \text{(VII.2)}$$

$$R(T) \leq r \leq R_0 \tag{VII.3}$$

where c_t is molar concentration of the diffusing matter, t is time, r represents radial position inside the fiber, R_0 stands for fiber radius, and $R_t = R(t)$ is the radial position of the diffusion surface, where $c(R,t) = 0$.

The material balance at the diffusion surface is presented as

$$D\frac{\partial c}{\partial r}(R,t) = -\frac{1}{2}bR \tag{VII.4}$$

Griffin and Coghanowr assume diffusivity, as well as concentration of the diffusing agent at the fiber surface [$c(R_0,t) = c_0 = const.$] to be constant. They assume also absence of convection in the filament. As a result the authors arrive at the following solution to the problem:

$$\begin{aligned} \frac{c_t}{c} = 1 - 2\left(\frac{b}{2c}\right)\int_{n=1}^{\infty}\frac{J_0(\lambda_n r/R_0)}{\lambda_n J_1(\lambda_n)} \times \exp\left(-\frac{\lambda_n^2 Dt}{R_0^2}\right) + \\ +\frac{b}{c_0}\sum_{n=1}^{\infty}\frac{J_0(\lambda_n r/R_{)})}{\lambda_n J_1(\lambda_n)}\frac{R}{R_0}\frac{J_1(\lambda_n R/R_0)}{J_1(\lambda_n)} - \\ -\frac{\lambda_n^2 D}{R_0^2}\int_0^t \frac{R'}{R_0}\frac{J_1(\lambda_n R'/R_0)}{J_1(\lambda_n)} \times \exp\left[-\frac{\lambda_m^2 D(t-t')}{R_0^2}\right] dt \end{aligned} \tag{VII.5}$$

where c_0 is molar concentration of the diluent around the filament, b is molar concentration of the polymer in the fiber, J_0 and J_1 are solutions of Bessel functions of zero and first order, respectively, and λ_n is an eigenvalue, $0 < \lambda_1 < \lambda_2 \ldots$ which are roots of $J_0(\lambda) = 0$.

From equation VII.5 describing concentration and from the condition $c(R,t) = 0$, result the two following equations which describe the moving boundary.

$$\begin{aligned} 1 = 2\left(\frac{b}{2c_0}\right)\sum_{n=1}^{\infty}\frac{J_0(\lambda_n R/R_0)}{\lambda_n J_1(\lambda_n)} \times \exp\left(-\frac{\lambda_n^2 Dt}{R_0^2}\right) + \\ +\frac{b}{c_0}\sum_{n=1}^{\infty}\frac{J_0(\lambda_n R/R_0)}{\lambda_n J_1(\lambda_n)} \times \phi_n \end{aligned} \tag{VII.6}$$

and

$$\begin{aligned} \frac{bR_0}{2c_0 D}\frac{dR}{dt} = -2\left(\frac{b}{2c_0}\right)\sum_{n=1}^{\infty}\frac{J_1(\lambda_n R/R_0)}{J_1(\lambda_n)} \times \exp\left(-\frac{\lambda_n^2 Dt}{R_0^2}\right) - \\ +\frac{b}{c_0}\sum_{n=1}^{\infty}\frac{J_1(\lambda_n R/R_0)}{J_1(\lambda_n)} \times \phi_n \end{aligned} \tag{VII.7}$$

where

$$\phi_n(R, R_0, D, t, \lambda_n) = \frac{\lambda_n^2 D}{R_0^2}\int_0^t \frac{R'}{R_0}\frac{J_1(\lambda_n R'/R_0)}{J_1(\lambda_n)} \times$$

$$\times \exp\left[-\frac{\lambda_n^2 D(t-t')}{R_0^2}\right] dt - \frac{R}{R_0}\frac{J_1(\lambda_n R/R_0)}{J_1 \lambda_n} \qquad \text{(VII.8)}$$

For long diffusion times, the first term in the solution of equations VII.6 and VII.7 has been given as

$$\frac{R_0 b}{2c_0 D}\frac{dR}{dt} = -\frac{\lambda_1 J_1(\lambda_1 R/R_0)}{J_0(\lambda_1 R/R_0)} \qquad \text{(VII.9)}$$

The equations are fit to be solved with use of a computer. If solving the problem *versus* time, it is possible to introduce corrections for changes of those parameters which were assumed constant at the derivation.

Equation VII.2 may be solved graphically,[23] if the accuracy of a graphic solution is sufficient. The relationship between the dimensionless parameters r/R and c_t/c_0 is presented in figure VII.1. The different lines in figure VII.1 correspond to another dimensionless parameter, Dt/R^2, values of which are given as parameter in the figure.

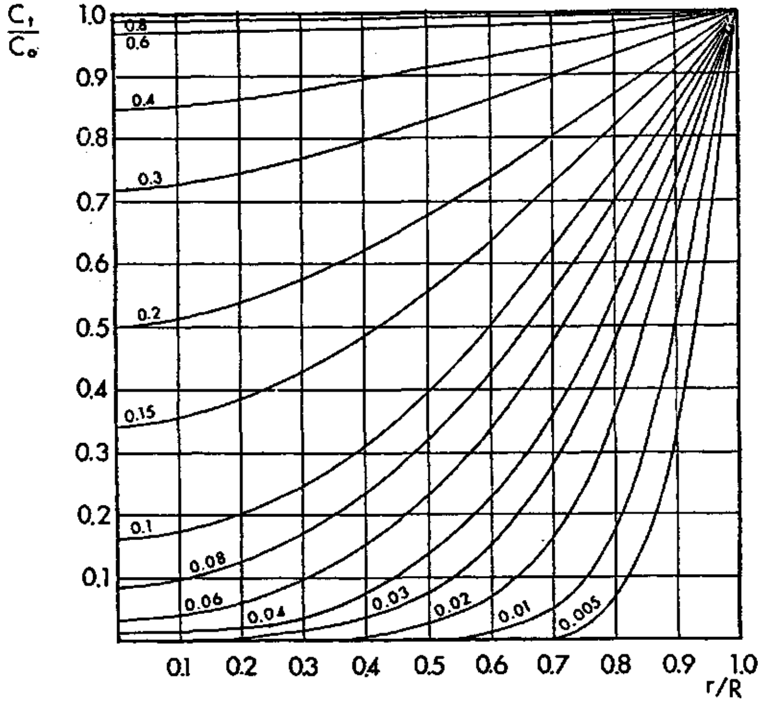

Figure VII.1: *Graphical solution of the equation for diffusion in a cylinder.*[23] *Explanation in text.*

If the values of c_0, c_t, t, and R are known from experiment, then from the graph in figure VII.1 one may read the values of the parameter Dt/R^2 corresponding to each r/R. For each value of r/R one may construct a separate plot between c_t/c_0

and the values of Dt/R^2, as read off the graph. From these graphs one may obtain the diffusivities, D.

In cases where the experimental data are available only for the average concentration across the diameter, solution is also possible, but is a little more laborious. One may assume that the whole area of the graph in figure VII.1 is equal to the amount diffused, c_0, until an equilibrium is established, that is, when $c_t = c_0$. In such a case, the amount which will diffuse in the given time, Dt/R^2, will be equal to the area under the corresponding curve and to the right of it, z_t. Then it is necessary to construct a plot of the ratio of the integrated areas, z_t over the total area z, as c_t'/c_0 against Dt/r^2. Here c is the average concentration of diffusant in a fiber cross section at time t. The further steps until obtaining the diffusivities are self evident.

Considering the diffusion in a wet process, A. Rende[22] assumed a different, somewhat more methodic approach. Namely, he considered two simultaneous diffusion processes: the diffusion of solvent out of the fiber, and the diffusion of the coagulant (nonsolvent) into the fiber. When the concentrations of polymer, solvent and nonsolvent overcome the phase equilibrium, coagulation takes place. This proceeds gradually from the filament surface toward the fiber axis, which results in a moving interface between the coagulated polymer in the outer layer and the uncoagulated dope inside.

At the first contact between the extruded filament and coagulation bath, a sudden desolvatation on the surface and the formation of a *skin* of coagulated polymer take place. This skin has different properties from the remainder of the fiber, even after the entire coagulation and drying process has been completed. The skin acts as a semipermeable membrane, such that no polymer passes through it but the low molecular mass solvent and non solvent diffuse. The volume ratio of the polymer, v_p, is considered constant during the entire process. It is also assumed that the filament is isotropic to the z-axis (along the fiber axis) and to θ – the angle in cylindrical coordinates.

Considering the above, the diffusion of solvent and coagulant are regarded as obeying Fick's law

$$\frac{dw_1}{dt} = -D_1\Omega_1\frac{dc_1}{da} \qquad \text{(VII.10)}$$

$$\frac{dw_2}{dt} = -D_2\Omega_2\frac{dc_2}{da} \qquad (VII.10\,a)$$

where w_j is the weight of the j^{th} species that entered the system, t is time, D_j coefficient of diffusion, Ω_j is diffusion surface area, and c_j stands for concentration of the j^{th} species in the filament at the radial distance a. The diffusion process is schematically presented in figure VII.2.

After a given time, t_1, the coagulant penetrates over a distance a_t radially from the skin. The concentrations c_1 and c_2 will reach their equilibrium values c_1* and c_2* at a distance a_1; in this way a_1 determines the position of the interface between the uncoagulated dope and coagulated polymer. Across the distance a_1, forms a gradient between the external c_{e1} and c_{e2} on one side, and c_1* and c_2* on

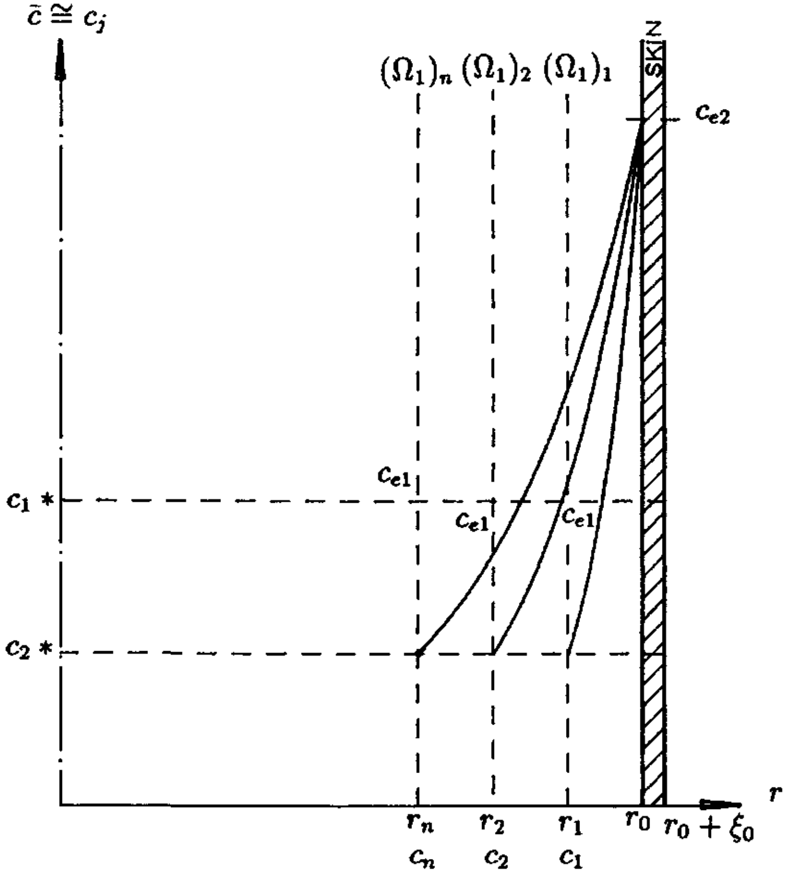

Figure VII.2: *Schematic representation of the diffusion process in a fiber.*

the other. After a time $t_2 > t_1$, the same process will be repeated on the radial distance $a_2 > a_1$.

As a consequence of this process, the diffusion surface, Ω_1, for the solvent will decrease as the process progresses.

$$\Omega_1 = 2\pi a z \tag{VII.11}$$

where, in agreement with Fick's law, a really means $a(t)$. The weight of the solvent passing through this surface is determined by the difference of the concentrations between the inner face and the external face of Ω_1, as well as by the time involved.

$$w_1 = \Delta c_1 \cdot \pi z(a_0^2 - a^2) \tag{VII.12}$$

where $a = a(t)$ and $\Delta c_1 = c_{e1} - c_1*$. And further

$$\frac{dw_1}{dt} = -2\pi z \Delta c_1 a \frac{da}{dt} \tag{VII.13}$$

For the coagulant Ω_2 is always the same and is the inner surface of the diffusion plane toward the interior of the filament.

$$\Omega_2 = 2\pi a_0 z \tag{VII.14}$$

where w_2 stands for the weight of the nonsolvent passing through the skin inside the filament, and it is determined as

$$w_2 = \Delta c_2 \pi z (a_0^2 - a^2) \tag{VII.15}$$

where $a = a(t)$ and $\Delta c_2 = c_{e2} - c_2*$, and further

$$\frac{dw_2}{dt} = -2\pi z \Delta c_2 a \frac{da}{dt} \tag{VII.16}$$

After substituting equations VII.12, VII.13, VII.14 and VII.16 into VII.10, one obtains

$$\Delta c_1 \frac{da}{dt} = -D_1 \; grad \; c_1 \tag{VII.17}$$

$$\Delta c_2 a \frac{da}{dt} = -D_2 a_0 \; grad \; c_2 \tag*{$(VII.17\,a)$}$$

Since the term da/dt, the *velocity of progress*, is the same for VII.17 and VII.17a, one may write

$$\frac{D_1}{\Delta c_1} \; grad \; c_1 = \frac{D_2}{\Delta c_2} \frac{a_0}{a} \; grad \; c_2 \tag{VII.18}$$

The analytical form of *grad* c_2 can be determined when $d\,w_2/dt = 0$. Physically, it determines *grad* c_2 across the uncoagulated filament at steady state. If one rewrites equation VII.15 using $\Delta c_2 = c_{e2} - c_2$, it results

$$\frac{dw_2}{dt} = 0 = \pi z \left[(c_{e2} - c_2) \frac{d}{dt}(a_0^2 - a^2) + (a_0^2 - a^2) \frac{d}{dt}(c_{e2} = c_2) \right] \tag{VII.19}$$

which on integration gives

$$\int_a^{\bar{a}} \frac{d(a_0^2 - a^2)}{(a_0^2 - a_2)} = - \int_{c_2}^{c_{i2}} \frac{d(c_{e2} - c_2)}{(c_{e2} - c_2)} \tag{VII.20}$$

In equation VII.20 we encounter for the first time $c_2 = c_{i2}$. The value of $\bar{a}$ in the integration limits means that a is the inner concentration of nonsolvent, After integration of VII.20 with the limit $\bar{a} \to 0$ one obtains

$$c_2 = c_{e2} - \Delta' c_2 \frac{a_0^2}{a_0^2 - a^2} \tag{VII.21}$$

In connection with equation VII.18, the concentration gradients may be calculated as

$$grad \; c_1 = -\frac{D_2}{D_1} \cdot \frac{\Delta c_1}{\Delta c_2} \cdot \frac{a_0^2}{a^2} \Delta' c_2 \frac{d}{da} \left(\frac{1}{a_0^2 - a^2} \right) \tag{VII.22}$$

$$grad\ c_2 = -a_o^2 \Delta' c_2 \frac{d}{da}\left(\frac{1}{a_0^2 - a^2}\right) \qquad (VII.22\,a)$$

where $\Delta c_j = c_{ej} - c_j*$ and $\Delta' c_j = c_{ej} - c_{ij}$ when c_{ij} stands for the inner concentration of the j^{th} species.

Equation VII.22 may be integrated with respect to a with limits as for equation VII.20 to yield c_1 as a function of c_{e1}, similarly as for c_2 in equation VII.21.

The velocity of coagulation (the *velocity of interface progression*), u, may be calculated from equations VII.22a and VII.17.

$$u = \frac{da}{dt} = -a_0^2 D_2 \frac{\Delta' c_2}{\Delta c_2} \cdot \frac{1}{a} \cdot \frac{d}{da}\left(\frac{1}{a_0^2 - a^2}\right) \qquad \text{(VII.23)}$$

The integral time required for complete coagulation is

$$t_c = \int u dt = \frac{a_0^2}{2} \cdot \frac{1}{D_2} \cdot \frac{\Delta c_s}{\Delta' c_2} \qquad \text{(VII.24)}$$

To solve equation VII.24, one needs the value of c_1*. To satisfy this, Rende[22] conducts the following considerations.

In view of the counterdiffusion of solvent and nonsolvent, a volume V_1 of solvent will leave the filament and a volume V_2 of nonsolvent will enter it. It is assumed that the total (original) volume of dope (filament) V_{tot} will remain constant, only a change of concentration takes place. When phase equilibrium point is reached, a phase separation into two phases with volumes $d \cdot V_{tot}$ and $c \cdot V_{tot}$, diluted and concentrated phases, respectively takes place. Naturally, $d + c = 1$. The volume fractions of the j^{th} species, v_j* in the total volume V_{tot} are related to the values of c_j* by $v_j* = c_j * /\rho_j$, where ρ_j is the density, and may further be given by the following equations.

$$\begin{array}{rcl} dv_1 + (1-d)v_1' & = & v_1 * \\ dv_2 + (1-d)v_2' & = & v_2 * \\ dv_p + (1-d)v_p' & = & v_p * \\ v_1 * + v_2 * + v_p * & = & 1 \end{array} \qquad \text{(VII.25)}$$

where v_j and v_j' represent the volume fractions on the j^{th} species in the diluted and concentrated fractions at the thermodynamic equilibrium, respectively.

It is assumed that at equilibrium the chemical potential μ of each species must be equal in both phases, that is

$$\mu_j = \mu_j' \qquad \text{(VII.26)}$$

where the subscript refers to the most concentrated phase.

According to Flory[32] these equations may be written as

$$\ln v_1 + (1 - v_1) - v_2 \frac{x_1}{x_2} - v_p \frac{x_1}{x_p} +$$

$$\begin{aligned} &+ && (\chi_{12}v_2 + \chi_{1p}v_p)(v_2 + v_p) - \chi_{2p}\frac{x_1}{x_2}v_2 v = \\ &= && \ln v_1' + (1 - v_1') - v_2'\frac{x_1}{x_2} - v_p'\frac{x_1}{x_p} + \\ &+ && (\chi_{12}v_2' + \chi_{1p}v_p')(v_2' + v_p') - \chi_{2p}\frac{x_1}{x_2}v_2' v_p' \end{aligned}$$

$$\begin{aligned} &\ln v_2 + (1 - v_2) - v_1\frac{x_2}{x_1} - v_p\frac{x_2}{x_p} + \\ &+ \quad (\chi_{21}v_1 + \chi_{2p}v_p)(v_1 + v_p) - \chi_{1p}\frac{x_2}{x_1}v_1 v_p = \\ &= \quad \ln v_2' + (1 - v_2') - v_1'\frac{x_2}{x_1} - v_p'\frac{x_2}{x_p} + \\ &+ \quad (\chi_{21}v_1' + \chi_{2p}v_p')(v_1' + v_p') - \chi_{1p}\frac{x_2}{x_1}v_1' v_p' \end{aligned} \tag{VII.27}$$

$$\begin{aligned} &\ln v_p + (1 - v_p) - v_2\frac{x_p}{x_2} - v_1\frac{x_p}{x_1} + \\ &+ \quad (\chi_{p2}v_2 + \chi_{p1}v_1)(v_2 + v_1) - \chi_{12}\frac{x_p}{x_2}v_2 v_1 = \\ &= \quad \ln v_p' + (1 - v_p') - v_2'\frac{x_p}{x_2} - v_1'\frac{x_p}{x_1} + \\ &+ \quad (\chi_{p2}v_2' + \chi_{p1}v_1')(v_2' + v_1') - \chi_{12}\frac{x_p}{x_2}v_2' v_1' \end{aligned}$$

where χ_{ij} is a pair interaction parameter, $\chi_{ij} = f(kT)^{-1}$; x_j describes the number of segments of the j^{th} species molecule.

The system is rather complicated, but may be simplified by the following assumptions: Both solvent and nonsolvent are monomeric compounds, so $x_1/x_2 = 1$. Further, $\chi_{ij} = \chi_{ji}(v_i/v_j)$, where V_i and V_j are molar volumes. Additionally, for polyacrylonitrile additional simplifications are valid:[22] for dimethyl formamide - water system $V_2 \cong 4V_1$, so $\chi_{12} = 0.25\chi_{21}$. Furthermore, $V_p \cong 10^4 V_2$ (or V_1), and in effect $x_1/x_p \cong x_2/x_p \cong 0$ and $\chi_{2p} = \chi_{p2} \cdot 10^{-4} \cong 0$. Lastly, $\chi_{1p} = 0$, therefore also $\chi_{p1} = 0$. For other solvent-nonsolvent systems similar simplifications may be possible.

Even with all the simplifications, the system of equations cannot be solved analytically; only numerical solutions are possible, but in the era of easily available fast desktop computers such tasks belong to accessible methods. Nevertheless, Rende[22] introduces still further simplifications.

One may admit that the more diluted phase does not contain any polymer, and the more concentrated phase consists only of the precipitated polymer. As a result $v_p = 0$; $v_p' = 1$; and $v_1' = v_2' = 0$. Consequently one may rewrite equations

VII.25 and VII.27, in a version for polyacrylonitrile, as

$$\begin{aligned} dv_1 &= v_1 * \\ dv_2 &= v_2 * \\ (1-d) &= v_p" \end{aligned} \tag{VII.28}$$

and

$$\begin{aligned} \ln v_1 + 0.25\chi_{21} v_2^2 &= \ln v_1' + 1 \\ \ln v_2 + \chi_{21} v_1^2 &= \ln v_2' + 1 \\ v_1 + v_2 &= 1 \end{aligned} \tag{VII.29}$$

Due to the approximately constant $V_{tot.}$ it results that $v_p = c_p/\rho_p$. Rende solved equations VII.29 by using the approximate series expansion of logarithms: $\ln(1+x) = x - x^2/2$. In this way the solution is

$$\frac{v_2}{1-v_2} = \frac{1 - sqrt1 - (1.5 - \chi_{21})(\chi_{12} + 0.5)}{\chi_{12} + 0.5} \tag{VII.30}$$

Rende[22] claims that the solution offered by equation VII.30 is "quite reliable", however, the values of χ_{21} must be determined experimentally, together with D_j, in the diffusion equations.

VII.3 Wet Process

In the wet process. we resort to the extraction of solvent by another liquid which is freely miscible with the solvent used, but it does not dissolve the polymer. The second liquid is usually called a *nonsolvent.* The depravation of the system of a sufficient amount of solvent leads to the coagulation of polymer. In another type of wet process, a polymer insoluble in any acceptable solvent is transformed chemically into a derivative which is soluble. Such a solution is extruded into a reactant, or a *nonsolvent* containing a reactant, which transforms the polymer chemically back to its original, insoluble form. The chemical reactions taking place in the coagulation bath may be taken as far as extruding a liquid *prepolymer*, which after extrusion is further polymerized to a high molecular mass solid polymer. Polyurethanes may serve here as an example.[24] Attempts have also been made to form fibers from emulsions instead of solutions.[24] Emulsions usually have much higher concentration of solids than solutions do. Viscosity of emulsions may be too low for good "spinnability", and increasing it to some necessary minimum level may be difficult without the use of auxiliaries adversely affecting important polymer properties.[14]

The concentrations of polymer solutions (*dopes*) used for fiber formation range rather widely, starting from about 3% all the way to 20% or possibly 30%. Processes are known which use much higher concentrations, all the way to a plasticized melt or semi-melt formation systems (40 to 60%) or so called *gel spinning*.[25–27] Concentration of the polymer solution used for fiber formation represents a major point in the economy of the process, thus the low concentrations may be applicable mainly for *high performance fibers* the customers of which may be willing to bear the extra high costs.

One may encounter opinions that the upper limit of concentration is limited by the high viscosity of solution and with the resulting difficulties to handle the high viscosity solutions. On the other hand, the physical properties of the resulting fibers improve with increasing solution concentration.[2] It seems, however, to be only partly true that high viscosity is the main obstacle here; melts of much higher viscosities are used with great success, fibers are formed from gels, so viscosity is not an unsurmountable problem. Use of low concentrations appears to be partially rooted in the tradition of formation from solution and partially in the difficulty of finding a solvent which would dissolve more polymer or fit all the other important requirements. The main reason for using solutions for fiber formation is the decomposition of a polymer at elevated temperature. The nature of wet processes is such that at higher temperatures, the high vapor pressure of the solvent may increase health and/or fire hazard beyond any acceptable level. The problem lies then in finding a solvent which gives sufficiently highly concentrated solutions at low temperature which is non-toxic and possibly easy to handle. Last, though not least for wet formation, a nonsolvent which is miscible and that also fulfills the other criteria valid for solvents must be available.

Theoretically speaking, mixed solvents can be used, but in practice it is very difficult to find such a mixture of solvents where the components would have similar diffusivities, and or evaporation rates. Azeotropes might be the best such possibility, but to find a suitable one may be even more difficult.

For design of spinnerettes the same general principles may be used as in case of melt spinning except that the pressures involved are most often correspondingly lower, so the plate thickness is smaller. In the majority of wet operations, the spinnerette is submerged in the coagulating bath and is connected by a transfer tube to the block containing the metering pump and filter assembly (see figure VII.3). The spacing between the spinnerette capillaries may be substantially smaller, as the easy access of the coagulating fluid provides sufficient antisticking protection.

Serkov and co-workers[11] have published an interesting study of fiber formation from polyacrylonitrile in dimethyl formamide as the solvent. The results of their investigations are presented in figures VII.4 and VII.5. The problems of diffusion were solved with the use of the graphic method[23] described in the preceeding section. The results are quoted here not because of the exactitude of the solution but because of the general idea of the time and distance scales of diffusion in the process.

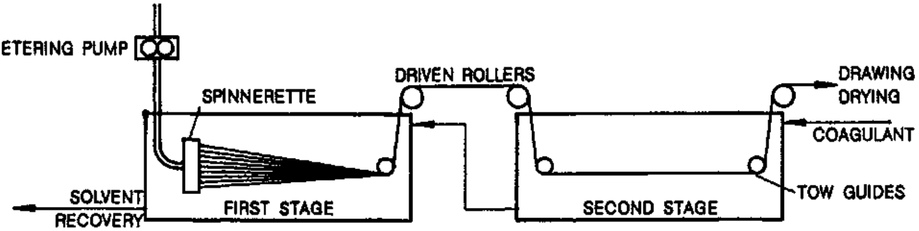

Figure VII.3: *Schematic representation of a wet process of fiber formation.*

In another publication Serkov and co-workers[47] determine diffusivity experimentally by placing a drop of solution between two glass Couette cylinders (or glass plates) and observe the flattened drop as it gradually precipitates (becomes hazy) upon introduction of nonsolvent between the glass surfaces. The necessary critical concentration for precipitation must be determined for a range of polymer concentrations, as there was found a strong dependence between the two parameters. The work was done with polyacrylonitrile dissolved in an aqueous solution of sodium thiocyanate.

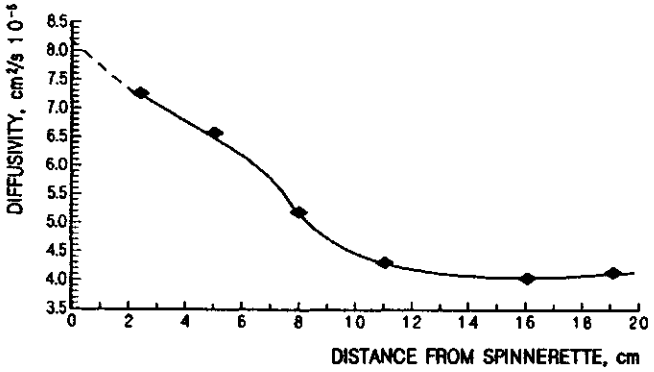

Figure VII.4: *Changes of diffusion coefficient for dimethyl formamide if polyacrylonitrile with distance from spinnerette. After Serkov et al.*[11]

As may be seen from figure VII.4, diffusivity is by no means constant, and in the quoted case it changes approximately by a factor of 2. This variability of diffusion coefficient casts serious doubts about the "wholesale solutions" suggested by some authors. A method to predict how diffusivity might change with increasing polymer concentration has been published by D. Machin and C. E. Rogers.[28] Their theory is based on comparison, analysis, and extension of free volume theories which were found mathematically equivalent. From this the authors have developed a method of determining diffusivity from the data on glass transition temperature.

Fujita and co-workers[33] have assumed that a penetrant requires a certain critical value, B_d, of free volume to promote diffusion and that the fraction of free volume, f, increases linearly with the volume fraction of the penetrant, Φ_1.

$$f = f_0 + \beta\Phi_1 \tag{VII.31}$$

where f_0 is the mean fractional free volume of pure polymer at a given temperature, $\beta = \gamma - f_0$ where γ is the corresponding fractional free volume of pure solvent. As generally $\gamma \gg f_0$ the diffusion coefficient D increases with Φ_1.

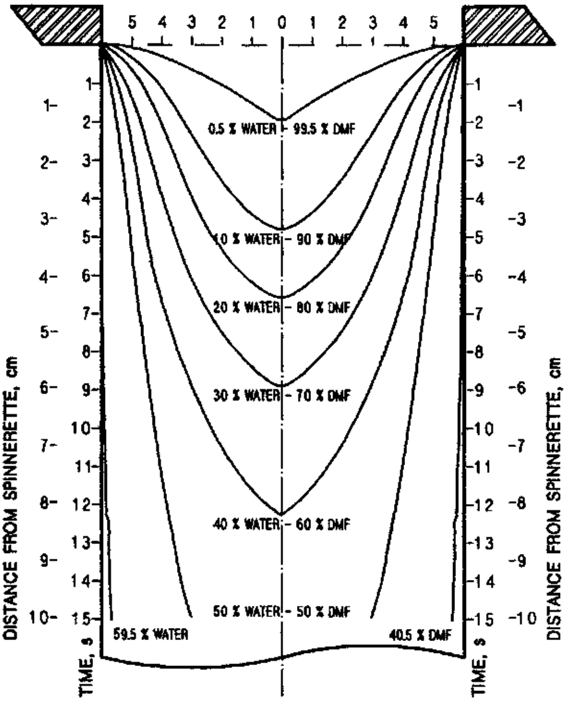

Figure VII.5: *Distribution of dimethyl formamide and water concentrations in a polyacrylonitrile fiber in relation to the distance from spinnerette and residence time in the coagulation bath. Extrusion velocity: 4m/min. After Serkov et al.*[11]

Further, the authors consider the theory by R. M. Vasenin[34] according to which a disturbance in a material is needed for the diffusing molecule to pass and this disturbance requires an energy ε. Further, Vasenin assumes that ε varies smoothly from ε_2^0 in pure polymer to ε_1^0 in a pure solvent according to a semiempirical relation.

$$\frac{-d\varepsilon}{d\Phi_1} = \frac{\beta'}{(1-\Phi_1)^2} \cdot (\varepsilon - \varepsilon_1^0) \tag{VII.32}$$

Another of Vasenin's relationships is:

$$\ln D = \ln D_0 + (\ln D_1 - \ln D_0)\left[1 - \exp\left(\frac{-\beta'\Phi_1}{1-\Phi_1}\right)\right] \tag{VII.33}$$

where D_1 is the diffusion coefficient in pure solvent. In the original work the physical meaning of β' was unclear; it was related to the plasticizing ability of the solvent.

The plots of $\ln D$ *versus* Φ_1 for solvents in glassy polymers show regions of changing curvature; these regions correspond the passage through the glass transition temperature. The calculations predict that such transitions should occur at Φ_1 lower than those observed experimentally. Under the assumptions that the energy ε varies smoothly with the composition below and above glass transition, equations analogous to equations VII.32 and VII.33 have been written.

$$\frac{d\varepsilon}{d\Phi_1} = -\frac{\beta_1'}{(1-\Phi_1)^2} \cdot (\varepsilon - \varepsilon_1^0) \qquad \text{(VII.34)}$$

$$\frac{d\varepsilon}{d\Phi_1} = -\frac{\beta_1'}{(1-\Phi_1)^2} \cdot (\varepsilon - \varepsilon_1^0) \qquad (VII.34\,a)$$

$$\ln D = \ln D_0 + (\ln D_1 - \ln D_0)\left[1 - \exp\left(\frac{-\beta_1'\Phi_1}{1-\Phi_1}\right)\right] \qquad \text{(VII.35)}$$

$$\ln D = \ln D_g + (\ln D_1 - \ln D_g)\left[1 - \exp\left(\frac{-\beta_2'(\Phi_1 - \Phi_g)}{(1-\Phi_1)(1-\Phi_g)}\right)\right] \qquad (VII.35\,a)$$

Equations VII.34 and VII.35 refer to the conditions below the glass transition and the versions "a" to conditions above glass transition. The equations open the possibility of a complete characterization of the diffusivities at $\Phi_1 = 0, \Phi_1 = 1$, at the transition, where are Φ_g and D_g, provided that the parameters β_1' and β_2' can be determined.

The measurements of the diffusivity below glass transition should be made in the steady state of diffusion to avoid the effects of slow polymer relaxation processes.

Fujita's theory has been expanded to cover a whole range of concentrations, not only the diluted ones, and to replace the linear dependence of free volume, f, on the volume fraction of the penetrant, Φ_1, with a more realistic function.

$$f = f_0 + F(\Phi_1, T) \qquad \text{(VII.36)}$$

where $F(1,T) = \gamma - f_0$.

Further, Machin and Rogers[28] take into account the equations relating glass transition temperature from the volume of the penetrant in four versions by four different authors, and so the equation by Fox:[35]

$$T_g = \frac{R_g^0 T_g^s}{\Phi_1(T_g^0 - T_g^s) + T_g^s} \qquad \text{(VII.37)}$$

by Kelly and Bueche:[36]

$$T_g = \frac{T_g^0 + \Phi_1 \cdot \left(\frac{\alpha_f^s}{\alpha_f^0} \cdot T_g^s - T_g^0\right)}{1 + \Phi_1 \cdot \left(\frac{\alpha_f^s}{\alpha_f^0} - 1\right)} \qquad \text{(VII.38)}$$

by Jenckel and Heusch:[37]

$$T_g = T_g^0 - \Phi_1(T_g^0 - T_g^s - K) - K\Phi_1^2 \tag{VII.39}$$

by Kanig:[38]

$$T_g = \frac{T_g^0 k \frac{(1-\Phi_1)}{\Phi_1} + T_g^s K - \frac{K_1}{1+\frac{\Phi_1}{k(1-\Phi_1)}}}{K + \frac{k(1-\Phi_1)}{\Phi_1}} \tag{VII.40}$$

In the above equations T_g^0 refers to the glass transition of a dry polymer, T_g^s is the glass transition of the solvent, α_f^0 and α_f^s are the differences in the thermal expansion coefficients above and below the glass temperature for the polymer and the solvent, respectively, $k = \alpha_f^s/\alpha_f^0$, K and K_1 are constants for the system, respectively.

The function $F(\Phi_1, T)$ from equation VII.36 has been derived as

$$f(\Phi_1, t) = \Phi_1 \left(\frac{A' + B'\Phi_1 + C'\Phi_1^2}{D' + E'\Phi_1 + F'\Phi_1^2} \right) \tag{VII.41}$$

The coefficients A', B', C', D', E', and F', and their dependence on the equation used for the calculation of glass transition temperature are given in table VII.1.

With the help of equation VII.41 one may calculate f from equation VII.36 and further estimate the relation

$$\frac{1}{\ln(D/D_0)} = \frac{f_0}{B_d} + \frac{f_0^2}{B_d} \cdot \left(\frac{D' + E'\Phi_1 + F'{\Phi_1}^2}{A' + B'\Phi_1 + C'{\Phi_1}^2} \right) \frac{1}{\Phi_1} \tag{VII.42}$$

The calculated functions

$$Y \left[\frac{1}{\ln(D/D_0)} - \frac{f\_0}{Bd} \right] \tag{VII.43}$$

and

$$Y \cdot \frac{\Phi_1}{\ln(D/D_0)} \tag{VII.44}$$

may be plotted *versus* Φ_1^{-1} and $Y\Phi_1$, respectively, where

$$f(\Phi_1, t) = \left(\frac{A' + B'\Phi_1 + C'\Phi_1^2}{D' + E'\Phi_1 + F'\Phi_1^2} \right)$$

If the obtained plots are linear, then it is an indication that the dependence between the diffusion and glass temperature is consistent. The value of f_0/B_d may be taken as the slope of $\Phi_1/[\ln(D/D_0)]$ *versus* Φ_1^{-1} for small Φ_1. In practice, it may be more convenient to evaluate graphically the relationship $F(\Phi_1, T)$ *versus* Φ_1 first, and then the D *versus* Φ_1. A high degree of accuracy may be obtained by this method.

Figure VII.5 presents the distribution of solvent and nonsolvent in a wet formed polyacrylonitrile fiber from the spinnerette on. The figure is drawn against time,

Table VII.1
Expression for constants in equation VII.41
and their dependence on source of T_g.[28]

Constant	Fox eqn. VII.37	Kelly & Bueche eqn. VII.38
A'	$\alpha_f^0({T_g^0}^2 - TT_g^s)$ $+\alpha_f^s T_g^s(T - T_g^0)$	$\alpha_f^s(T - T_g^s)$ $+\alpha_f^0(T_g^0 - T)$
B'	$T(T_g^0 - T_g^s)$ $(\alpha_f^s - \alpha_f^0)$	$\alpha_f^s(\alpha_f^s - \alpha_f^0)/\alpha_f^0$ $\times(T - T_g^s)$ $+(T_g^0 - T)(\alpha_f^s - \alpha_f^0)$
C'	0	0
D'	T_g^s	1
E'	$T_g^0 - T_g^s$	$\frac{\alpha_f^s}{\alpha_f^0} - 1$
F'	0	0

Constant	Jenckel & Keusch eqn. VII.39	Kanig eqn. VII.40
A'	$\alpha_f^0(2T_g^0 - T - T_g^0 - K)$ $+\alpha_f^s(T - T_g^0)$	$\alpha_f^0(KT_g^0 - KT_g^s - K_1)$ $+\alpha_f^s/\alpha_f^0$
B'	$\alpha_f^0(2K - T_g^0 + T_g^s)+$ $+\alpha_f^s(T_g^0 - T_g^s - K)$	$\alpha_f^0[2K_1 + K(T_g^0 - T_g^s)$ $\times(\alpha_f^0/\alpha_f^s - 2)]$ $+\alpha_f^s[K(T_g^0 - T_g^s)$ $-K_1 - \alpha_f^s/\alpha_f^0] + [1 + K]$
C'	$K(\alpha_f^s - \alpha_f^0)$	$k\left(\frac{\alpha_f^0}{\alpha_f^s} - 1\right) + \left(\frac{\alpha_f^s}{\alpha_f^0} - 1\right)$ $-K(T_g^0 - T_g^s)(\alpha_f^s - \alpha_f^0)^2/\alpha_f^s$
D'	1	α_f^s/α_f^0
E'	0	$1 + K - \frac{2\alpha_f^s}{\alpha_f^0}$
F'	0	$K\left(\frac{\alpha_f^0}{\alpha_f^s} - 1\right) + \left(\frac{\alpha_f^s}{\alpha_f^0} - 1\right)$

and distance scale is also given. The slowness of the diffusion process may be here well appreciated; the consequences of the low rate of fiber formation in a wet process do not need any more emphasis.

When ions are present in the dope and/or the coagulating bath, like in processes involving water type solvents, *e. g.* rayon processes, cuprammonium, or sodium thiocyanate, the diffusion may be additionally complicated by the interphase potential.[63] The diffusion potential, $\Delta\phi$, between two phases, a and b, may be described by the Henderson equation.

$$\Delta\phi = \phi_a - \phi_b = \frac{RT}{F}\frac{\sum z_i\omega_i[c_i(b) - c_i(a)]}{\sum z_i^2\omega_i[c_i(b) - c_i(a)]} \times \ln\left[\frac{\sum z_i^2\omega_i c_i(a)}{\sum z_i^2\omega_i c_i(b)}\right] \qquad \text{(VII.45)}$$

where ω_i is molar mobility of the species i, z_i is charge of the species i, c_i is concentration of the species, and A is the interphase area. The equation gives a fair agreement with the majority of ions involved in formation of the cellulosic fibers.

In the presence of electrical potential between phases, the flux of the ion species, J_i, is described by the Nernst-Planck equation.

$$J_i = -\omega_i RT \times \left(\frac{dc_i}{dx}\right) - z_i F \omega_i c_i \times \left(\frac{d\phi}{dx}\right) \tag{VII.46}$$

The ion flux, as given by equation VII.46, depends on the interphase potential. In processes of wet fiber formation involving ions, the rate of coagulation would, certainly, depend on the ion flux.

From the point of view of fiber properties, it is beneficial to have the diffusion process less drastic, slower. The different nonsolvents have different precipitation powers, so for the full precipitation of certain volume of polymer solution, different volumes of nonsolvent may be needed, depending on the physico-chemical nature of the nonsolvent. For this reason it is customary to have a lower precipitating power close to the spinnerette, and to increase it gradually along the moving tow. Usually this is achieved by using a mixture of solvent and nonsolvent as the precipitating bath. The concentration of nonsolvent should increase as the degree of fiber coagulation increases.

Additionally, to provide for some concentration gradient in the coagulation process along the path of the fiber travel, the coagulation bath is pumped either counter- or co-current to the movement of fibers, To facilitate the transport of coagulation medium, the fibers are often led through several baths of increasing precipitant concentration. This, however, does not solve, nor describe the whole problem. The strength of a nonsolvent may sometimes be changed by some additives or by change of pH. For example, pH of the mixture of water and dimethyl formamide (DMF) used to precipitate poly(acrylonitrile) from DMF solution has a strong influence on the precipitating power at the same solvent-nonsolvent concentration. The effect of pH on the cross section of poly(acrylonitrile) fibers coagulated in a water - dimethyl formamide mixture may be seen in figure VII.6.[15] The stronger the deformation of the circular cross section of the fiber, the more drastic is the precipitation.

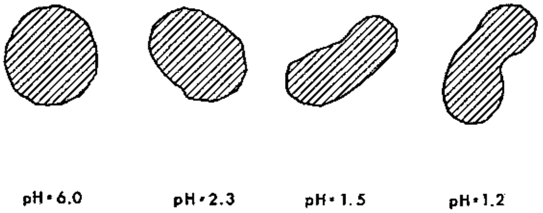

Figure VII.6: *Cross sections of fibers obtained in a wet processes with coagulants of different strength; the strength increased with decreasing pH. After Gröbe and Gieske.*[15]

The filament surface, as it moves through the coagulation bath, does have some boundary layer across which is a gradient of solvent - nonsolvent concentration. Griffith[29] has developed an approximate analytical solution to the changes of concentration, or temperature, in the radial direction from the inside of the filament out into the fluid. The approximation is based on the following assumptions: constant filament diameter, the filament moves at an uniform (constant) velocity, and the fluid in which the fiber moves is homogeneous. The final solution for the concentration changes is suggested as

$$c* = \frac{c_t - c_0}{c_{f0} - c_0} = \int_0^\infty \exp\left[-\left(\frac{lD}{Rv_f}\right)u^2\right] J_0(u,r)J_1(u)du \qquad \text{(VII.47)}$$

where $c*$ is concentration, c_t is bath concentration, c_0 is initial bath concentration, c_f stands for initial concentration in the fiber at the distance from spinnerette of l expressed in the units of R, where R is filament radius, D represents mass diffusivity, v_f is filament velocity, u stands for medium velocity divided in v_f. J_0 and J_1 are Bessel functions of zero and first order, respectively.

An analogous equation for temperature changes in the radial direction r is

$$T* = \frac{T_t - T_0}{T_{f0} - T_0} = \int_0^\infty \exp\left[-\left(\frac{l\alpha}{Rv_f}\right)u^2\right] J_0(u,r)J_1(u)du \qquad (VII.47\,a)$$

In analogy to the equation for concentration, T_t means the medium temperature, T_0 is the initial medium temperature, T_{f0} is initial filament temperature, and α is thermal diffusivity.

The solution of equation VII.47 and VII.47a is given in the form of a graph in figure VII.7. The different curves given in the graph represent the radial distance from the filament axis in units of filament radius, R, as indicated in the figure. For an average wet spinning operation, the graph given in figure VII.6 covers some 15 to 20 cm distance from the spinnerette before the different curves join together. Velocity profile in the fluid may be estimated from the boundary layer theory suggested by Sakiadis and described in section VI.1.b, or by using any of the experimental relationships.

In today's era of the computer, numerical solutions are preferred and easily available, though the approximate graphical solution of figure VII.7 may be used for quick rough estimates if the proper computer programs are not available.

It is intuitively quite obvious that in the nearest vicinity of a wet formed filament, throughout the boundary layer, the concentrations of solvent and nonsolvent are not constant; there are gradients, and the gradients are not necessarily constant. The motion of the filament also must be expected to affect those concentration gradients. G. A. Danilin[40] has devoted some attention to the problem and in effect he published a group of equations to calculate those effects.

Danilin uses the following definition of the used symbols: x and y are the cylindrical coordinates for the system, the first one coinciding with the fiber axis; u and v are projections of the precipitating bath velocities in the boundary layer on the x and y axes, respectively; u_s and v_s are the values of u and v on the filament surface; u_e is the value of u at the outer edge of the boundary layer, it is

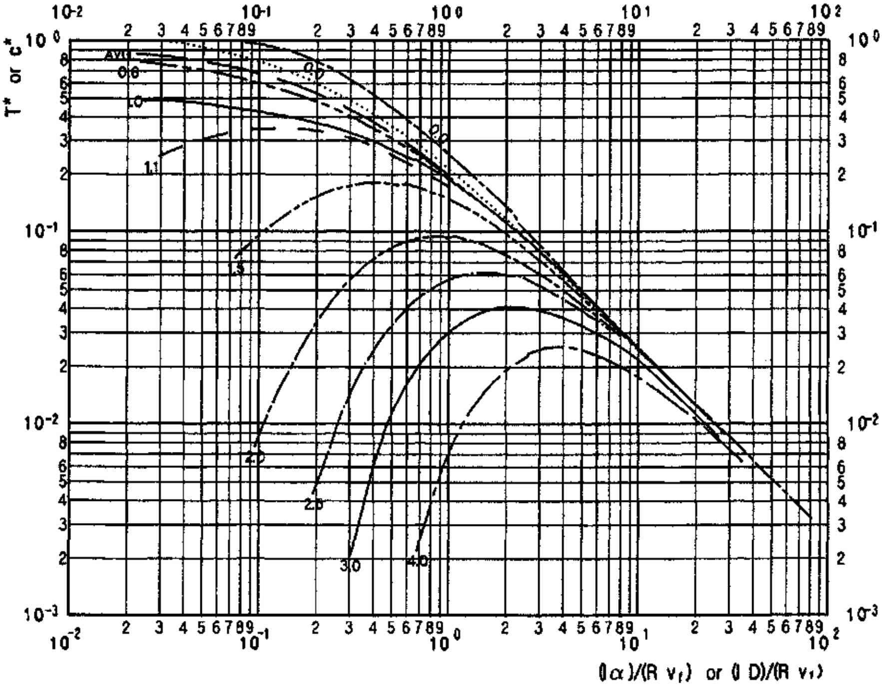

Figure VII.7: *Temperature, or concentration, inside and outside of a filament during the wet formation, as calculated according to equation VII.45 or VII.45a. After R. M. Griffith.*[29]

the lengthwise velocity of the coagulation bath; ν is the kinematic viscosity of the coagulation bath; c and c_1 are the concentrations of solvent in the bath and the initial concentration in the fiber (dope); c_e is the initial concentration of solvent in the coagulation bath; D and D_1 are the diffusion coefficients of the solvent in the precipitating bath and in filament and usually $D \neq D_1$; K is distribution coefficient; ρ_1 is the density of the solvent exiting the filament; α represents the angle between the tangent to the generatrix of the filament surface and x-axis, it describes the local rate of diameter reduction; V_p^* is the projection of the velocity of the liquid exiting the filament onto the normal to the fiber surface; Q is the volumetric flow rate of the polymer solution at a distance from spinnerette. The relationships describing the problem, as well as the boundary conditions are given as follows:

$$\frac{\partial yu}{\partial x} + \frac{\partial yv}{\partial y} = 0 \qquad \text{(VII.48)}$$

$$u\frac{\partial u}{\partial x} + v\frac{\partial u}{\partial y} = u_e\frac{\partial u_e}{\partial x} + \frac{v}{y} \cdot \frac{\partial}{\partial y}\left(y\frac{\partial u}{\partial y}\right) \qquad \text{(VII.49)}$$

$$u\frac{\partial c}{\partial x} + v\frac{\partial c}{\partial y} = \frac{D}{y} \cdot \frac{\partial}{\partial y}\left(y\frac{\partial c}{\partial y}\right) \qquad \text{(VII.50)}$$

$$u_1 \frac{\partial c_1}{\partial c} \partial x - \frac{y}{2} \cdot \frac{\partial u_1}{\partial x} \cdot \frac{\partial c_1}{\partial y} = \frac{D_1}{y} \cdot \frac{\partial}{\partial y} \left(y \frac{\partial c_1}{\partial y} \right) \tag{VII.51}$$

$$u = u_s = u_1 + \frac{V_p}{\cos \alpha} \left(1 - \frac{\rho_1}{\rho} \right) \cos \alpha \cdot \sin \alpha \tag{VII.52}$$

$$v = v_s = u_s \tan \alpha + \frac{\rho_1 V_p}{\cos \alpha} \tag{VII.53}$$

if $c = Kc_1$ and for $y = R$ and $x \geq 0$ then

$$\rho_1 D_1 \frac{\partial c_1}{\partial y} = \rho D \frac{\partial c}{\partial y} + \frac{\rho_1 V_p}{\cos \alpha} \cdot (c_1 - c) \tag{VII.54}$$

$$\begin{gathered} u = u_e \text{ and } c = c_e \text{ if } R < y < \infty \text{ and } x = 0 \\ c_1 = c_1^0 \text{ if } 0 \leq y < R \text{ and } x = 0 \\ u \to u_e \text{ and } c \to c_e \text{ when } y \to \infty \text{ and } x > 0 \\ \text{when } y = 0 \text{ and } x > 0 \text{ then } \tfrac{\partial c_1}{\partial y} = 0 \end{gathered}$$

And further definitions are:

$$\tan \alpha = \frac{dR}{dx} \tag{VII.55}$$

$$\frac{\rho_1 V_p}{\cos \alpha} = -\frac{1}{2\pi R} \cdot \frac{d}{dx} \tag{VII.56}$$

$$\text{when} \quad q = \rho_1 Q \text{ and } Q = \pi R^2 u_1.$$

To solve the equations VII.48 through VII.56, one needs to have the information on the change of fiber velocity in the bath (u_1) and the volumetric flow rate of the spinning dope, Q, as a function of the process parameters.

The author[40] indicates, however, that in the real processes, the equality of the velocity components of the bath and filament does not occur, $u_s \neq u_1$. The last inequality would hold true if the densities of bath and fiber surface were equal, $\rho_1 = \rho$, or if there were no mass flow on the filament surface, $V_p = 0$. Nevertheless, the author claims that in real processes, despite the fact that $\rho_1 \neq \rho$ and $V_p \neq 0$, the values of the component velocities are very close, so in the first approximation they may be taken as equal, $U_s = u_1$.

With a more complete process analysis the equations given by Danilin may be solved, though the task is not exactly easy. However, no simpler method is available.

In commercial operations of wet formation of fibers, the number of filaments extruded from one spinnerette is very large, reaching several tens of thousands. The dense bundle of filaments presents an obstacle for the coagulation bath to penetrate inside the tow. An attempt to describe the problem has been published by Szaniawski and Zachara.[30,31] As the problem is quite complex, the authors make the following simplifying assumptions: The interior of the fiber bundle is taken as uniformly anisotropic porous medium in which the fluid flows according to the Darcy's law. The coagulating fluid is taken as homogeneous, viscous, and with constant density. The fibers are taken as rigid cylindrical rods. The mass exchange and the influence of gravity are neglected. Flat and cylindrical geometries of the tow are considered.

When we designate as A the cross section of the tow, as N the number of filaments in the tow, as d filament diameter, and as s cross section of a filament, then one may define the ratio of the volume of fibers to the volume of the tow as

$$\varphi = \frac{\pi d^2}{4s} \tag{VII.57}$$

where $s = A/N$. In typical cases $\varphi < 0.05$, or generally $\varphi \ll 1$. Considering the slow flow of fluid one may apply Darcy's law in the form

$$w_{\|} = -\frac{s}{\eta} \cdot F_{\|}(\varphi) \cdot grad_{\|} p \tag{VII.58}$$

$$w_{\perp} = -\frac{s}{\eta} \cdot F_{\perp}(\varphi) \cdot grad_{\perp} p \tag{$VII.58\,a$}$$

where $w_{\|}$ and $w\perp$ are the components of filtration velocity in parallel and in perpendicular directions, respectively, and correspondingly parallel and perpendicular to the fiber axis: p – pressure, η – dynamic viscosity of fluid, $F_{\|}$ and $F_{\perp}$ – coefficients of filtration resistance.

As the velocity of filtration, $\vec{w}$, we define the output of fluid which flows through a unit of porous surface in relation to this surface. Generally, the linear Darcy's law is applicable up to the Reynolds number $Re < 10$, though the limit is not well defined and for Reynolds numbers somewhat over 10 it may still give acceptable results. For this case, the Reynolds number is defined as

$$Re_d = \frac{|w|d}{\mu} \tag{VII.59}$$

Here $|w|$ denoted the modulus of the filtration velocity, μ is kinematic viscosity.

The coefficients of filtration resistance, $F_{\|}$ and $F_{\perp}$, basically depend on φ and on the configuration of fibers in the considered space. However, since φ is very small, one may take advantage of the simplified relationship which does not depend on the configuration.

$$F_{\|} = 2F_{\perp} = \frac{1}{4\pi} \cdot \left[\ln\left(\frac{1}{\varphi}\right) - 1.5\right] \tag{VII.60}$$

In the case of a flat tow, the problem is considered in the Cartesian coordinates, with cylindrical tow, cylindrical coordinates are to be used. The axis $x - o$ is on the surface of the spinnerette, while the axis $o - z$ is parallel to the fiber axis. In such coordinates, Darcy's law has the form

$$u_z - v \cdot (1 - \varphi) - \frac{s}{\eta} \cdot F_{\|} \frac{\partial p}{\partial z} \tag{VII.61}$$

$$u_x = w_x = -\frac{s}{\eta} \cdot F_{\perp} \frac{\partial p}{\partial x} \tag{$VII.61\,a$}$$

Here $w_x = w_\perp$ and $w_z = w_\parallel$ are the components of the fluid velocity in relation to the tow; u_x and u_z are the components of the velocity of fluid in the static system connected with the spinnerette.

In view of the assumed constant fluid density and neglected mass exchange, the continuity equation may be written as

$$\frac{\partial w_z}{\partial z} + \frac{\partial w_z}{\partial x} + k\frac{w_x}{x} = 0 \tag{VII.62}$$

where $k = 0$ for flat tow, and $k = 1$ for cylindrical tow with axial symmetry.

When we substitute into equation VII.62 the values for w_x and w_z as obtained from equation VII.61, and take into account that $\eta, s, F_\parallel, F_\perp$ do not depend on x or z, we obtain the equation for the pressure

$$\frac{F_\parallel}{F_\perp} \cdot \frac{\partial^2 p}{\partial z^2} + \frac{\partial^2 p}{\partial x^2} + \frac{k}{x} \cdot \frac{\partial p}{\partial x} = 0 \tag{VII.63}$$

The boundary conditions for equation VII.63 are as follows: On the axis of symmetry $x = 0$, the transverse velocities are equal zero, $u_x = w_x = 0$. At the spinnerette ($z = 0$) $u_z = 0$ and at a large distance from the spinnerette ($z \longrightarrow \infty$) the fluid velocity reaches the velocity of fibers ($w_z = 0$). Considering all these and equation VII.63, one obtains the following relationships

$$\frac{\partial p(0,z)}{\partial x} = 0 \tag{VII.64}$$

$$\frac{\partial p(x,0)}{\partial z} = \frac{v\eta(1-\varphi)}{sF} \tag*{(VII.64 a)}$$

$$\lim_{z \to \infty} p(x,z) = const. \tag*{(VII.64 b)}$$

On the surface of the tow ($x = \pm a$), one needs to take into account the mutual interaction of both areas of flow. Under the assumption that outside the tow the flow resistance is relatively small, one may use Bernoulli's equation

$$p + \frac{\rho}{2} \cdot (u_x^2 + u_z^2) = p_0 \tag{VII.65}$$

where ρ is fluid density and p_0 is the pressure of stagnation. This condition the authors consider in two versions:

$$p(a,z) - p_0 = 0 \qquad \text{version 1} \tag{VII.66}$$

$$p(a,z) - p_0 = \frac{\rho u_x^2}{2} \qquad \text{version 2} \tag*{(VII.66 a)}$$

In version VII.66, the influence of dynamic pressure has been neglected, while in version VII.66a only the main part of the dynamic pressure, $\rho u_x^2/2$, has been taken into account and the segment $\rho u_z^2/2$ has been omitted.

Upon introduction of dimensionless variables

$$\xi = \frac{x}{a} \tag{VII.67}$$

$$\zeta = \sqrt{\frac{F_{\perp}}{F_{\parallel}}} \cdot \frac{z}{a} \tag{VII.67 a}$$

$$\Pi = \frac{s}{\eta} \sqrt{F_{parallel} \cdot F_{perp}} \cdot \frac{p - p_0}{v(1-\varphi)a} \tag{VII.67 b}$$

the problem is reduced to the finding of a function which would fulfill Laplace's equation

$$\frac{\partial^2 \Pi}{\partial \zeta^2} + \frac{\partial^2 \Pi}{\partial \xi^2} + \frac{k}{\xi} \cdot \frac{\partial \Pi}{\partial \xi} = 0 \tag{VII.68}$$

and the boundary conditions

$$\frac{\partial \Pi(0,\zeta)}{\partial \xi} = 0 \tag{VII.69}$$

$$\frac{\partial \Pi(\xi,0)}{\partial \zeta} = 1 \tag{VII.69 a}$$

$$\lim_{\zeta \to \infty} \Pi(\xi,\zeta) = 0 \tag{VII.69 b}$$

$$\Pi(1,\zeta) = 0 \qquad \text{version 1} \tag{VII.69 c1}$$

$$\Pi(1,\zeta) = -\varepsilon \left[\frac{\partial \Pi(1,\zeta)}{\partial \xi} \right]^2 \qquad \text{version 2} \tag{VII.69 c2}$$

In the last equation, the authors introduced a nondimensional parameter ε, which is defined as

$$\varepsilon = \frac{Re}{N}(1-\varphi)F_{\perp}\sqrt{\frac{F_{\perp}}{F_{\parallel}}} \tag{VII.70}$$

where

$$Re = \frac{vA}{2a\mu} \tag{VII.70 a}$$

The Reynolds number defined with the equation VII.70a is related to the whole tow and is different from that defined with the equation VII.59, Re_d, which pertains to a filament and depends on the location in space.

Upon finding the function $\Pi(\xi,\zeta)$ and using equations VII.63 and VII.59, one may describe the flow conditions by calculating the field of flow parameters $p(x,z), u_x(x,z), u_z(x,z)$, as well as calculate the streamlines in relation to the system moving with the tow, or in relation to the spinnerette. Using nondimensional variables, the equations of the streamlines for both systems have the form

$$\tilde{q} = \int (k+1)\xi^k \left(\frac{\partial \Pi}{\partial \xi} d\zeta - \frac{\partial \Pi}{\partial \zeta} d\xi \right) = const. \tag{VII.71}$$

$$q = \xi^{k+1} + \tilde{q} = const. \qquad (VII.71\,a)$$

where the nondimensional functions q and $\tilde{q}$ are proportional to the flow intensity of the fluid as it flows between the surfaces located symmetrically to the axis.

Analytical solution of equation VII.68 for cylindrical tow (version VII.66a) has been found unsatisfactory, thus the equation must be solved numerically. The calculated results give good insight into the studied problem and are reproduced in figures VII.8 and VII.9.

A satisfactory analytical solution has been found by Szaniawski and Zachara[31] for a flat tow with a pressure differential on both sides of the tow. The nondimensional pressure drop is

$$\Pi(\xi,\zeta) = \frac{8}{\pi^2}\sum_{n=1}^{\infty}\frac{(-1)^n}{(2n-1)^2}\cdot\exp\left[-\frac{(2n-1)\pi\zeta}{2}\right]\cdot\cos\left[\frac{(2n-1)\pi\xi}{2}\right] \qquad \text{(VII.72)}$$

Pressure distribution is presented as

$$\tilde{\Pi}(\xi,\zeta) = \frac{\left(p - \frac{p_- + p_+}{2}\right)}{p_0} = \bar{\Pi}\cdot\xi + \Pi(\xi,\zeta) \qquad \text{(VII.73)}$$

where

$$\bar{\Pi} = \tilde{\Pi}(1,\zeta) = \frac{(p_+ - p_-)}{2p_0} \qquad (VII.73\,a)$$

For $\bar{\Pi} = 0$ is $\tilde{\Pi} = \Pi$.

The knowledge of the pressure field allows us to calculate from equation VII.61 the field of filtration velocity u_x, u_z. After integration of the equation of streamline $dx/u_x = dz/u_z$ one obtains the nondimensional function of stream

$$q(\xi,\zeta) = \frac{Q}{v(1-\varphi)a} = \xi + \bar{\Pi}\cdot\zeta + \tilde{q}(\xi,\zeta) \qquad \text{(VII.74)}$$

where function $\tilde{q}$ has the form

$$\tilde{q}(\xi,\zeta) = \frac{8}{\pi^2}\sum_{n=1}^{\infty}\frac{(-1)^n}{(2n-1)^2}\cdot\exp\left[-\frac{(2n-1)\pi\zeta}{2}\right]\cdot\sin\left[\frac{(2n-1)\pi\xi}{2}\right] \qquad \text{(VII.75)}$$

Q represents the volume of fluid flowing in the area between the spinnerette and a given streamline $q = const.$

Some additional equations connected to the problem are: Pressure on the surface of the spinnerette at the point $\xi = \zeta = 0$

$$\tilde{\Pi}(0,0) = \Pi(0,0) = -\frac{8\cdot G}{\pi^2} = -0.7424... \qquad \text{(VII.76)}$$

where G represents the constant of Catalan.

The coordinate ξ on the spinnerette where the pressure is at a minimum $\bar{\Pi}(\xi_2, 0) = \bar{\Pi}_{min.}$ and the streamline $q = 0$ looses contact with the spinnerette surface is defined as

$$\xi = \frac{4}{\pi} \arctan\left[\exp\left(-\bar{\Pi}\frac{\pi}{2}\right)\right] - 1 \qquad \text{(VII.77)}$$

The coordinate of the point where the border streamline would be tangent to the surface of the tow and the stream function reaches a minimum $q(-1, \zeta_1) = q_{min.} < 0$ is given as

$$\zeta_1 = \frac{2}{\pi} \cdot \ln\left[\frac{\exp\left(\frac{\pi}{2}\bar{\Pi}\right) + 1}{\exp\left(\frac{\pi}{2}\bar{\Pi}\right) - 1}\right] = \frac{2}{\pi} \ln\left[\coth\left(\pi\bar{\Pi}\right)\right] \qquad \text{(VII.78)}$$

The results of the pressure and streamline calculations are presented in figure VII.10 and VII.11.

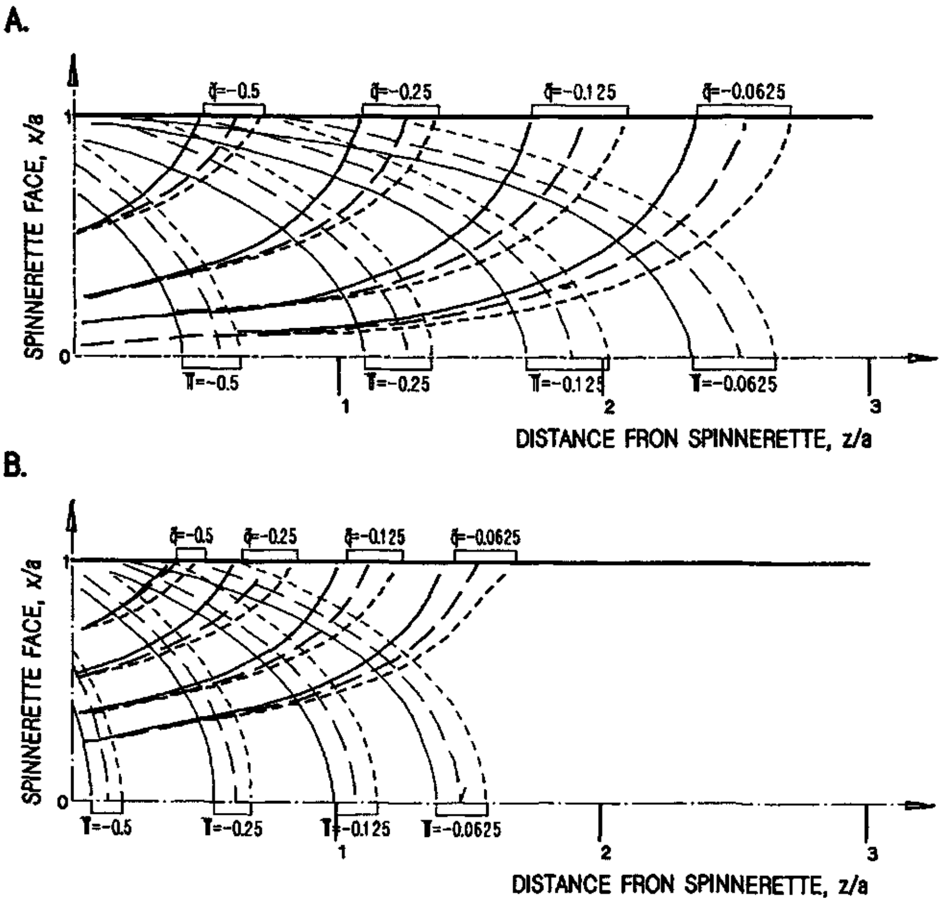

Figure VII.8: *Cylindrical tow. Isobars* (Π = *const.*) *and streamlines* ($\tilde{q}$ = *const.*); *A – flat tow, B – cylindrical tow. Full drawn line* $\varepsilon = 0$, *dashed line* $\varepsilon \approx 0.1$, *short dashed line* $\varepsilon = 0.2$. *After A. Szaniawski and A. Zachara.*[30]

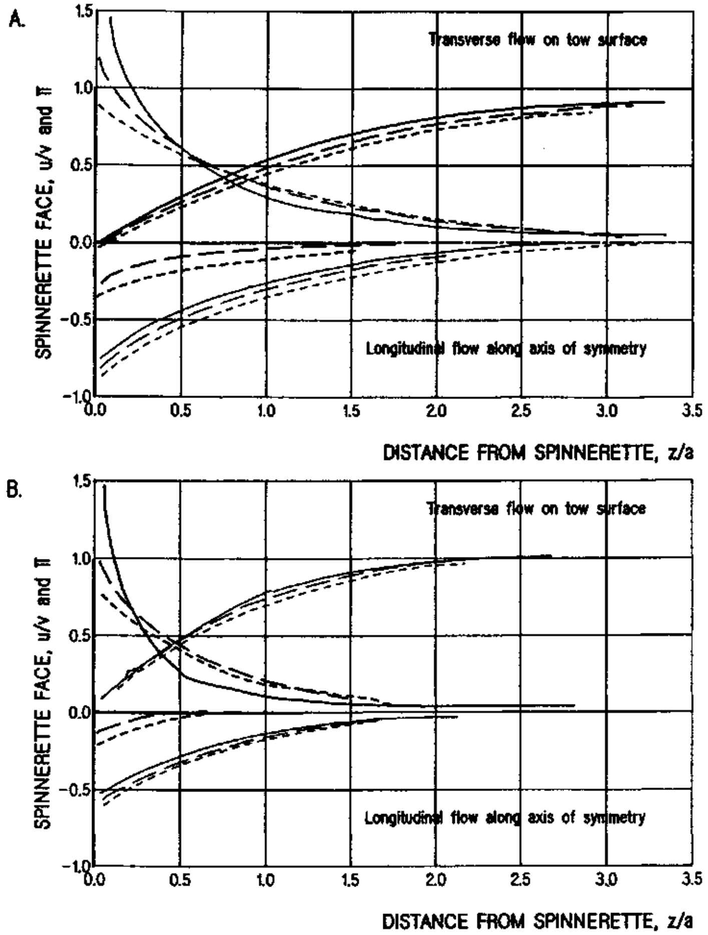

Figure VII.9: *Cylindrical tow. Fluid velocities in tow: Top of graph: transverse flow,* (u_x/v)*, on the surface,* $(x = a)$*, and longitudinal flow,* (u_z/v)*, on the axis of symmetry,* $(x = 0)$*. Bottom of graph: pressure drop on the surface and on the axis of symmetry. Full drawn line* $\varepsilon = 0$*, dashed line* $\varepsilon = 0.1$*, dotted line* $\varepsilon = 0.2$*. A - flat tow, B - cylindrical tow. After A. Szaniawski and A. Zachara.*[30]

The derivations proposed by Szaniawski and Zachara[30,31] and quoted above may be useful also for solution of similar problems encountered with the flow of quench air in the fiber formation from melt or in the dry formation from solution.

The extrusion temperature has a strong and multilateral influence on the process performance and on the resulting product. It, together with concentration, determines the solution viscosity, coefficient of diffusivity, and interaction with the nonsolvent used. Often, fiber density increases with the increasing temperature of the processing.[39] High density with strong skin effect, also depending on temperature and diffusivity, may cause difficulties with subsequent drying of the fibers.

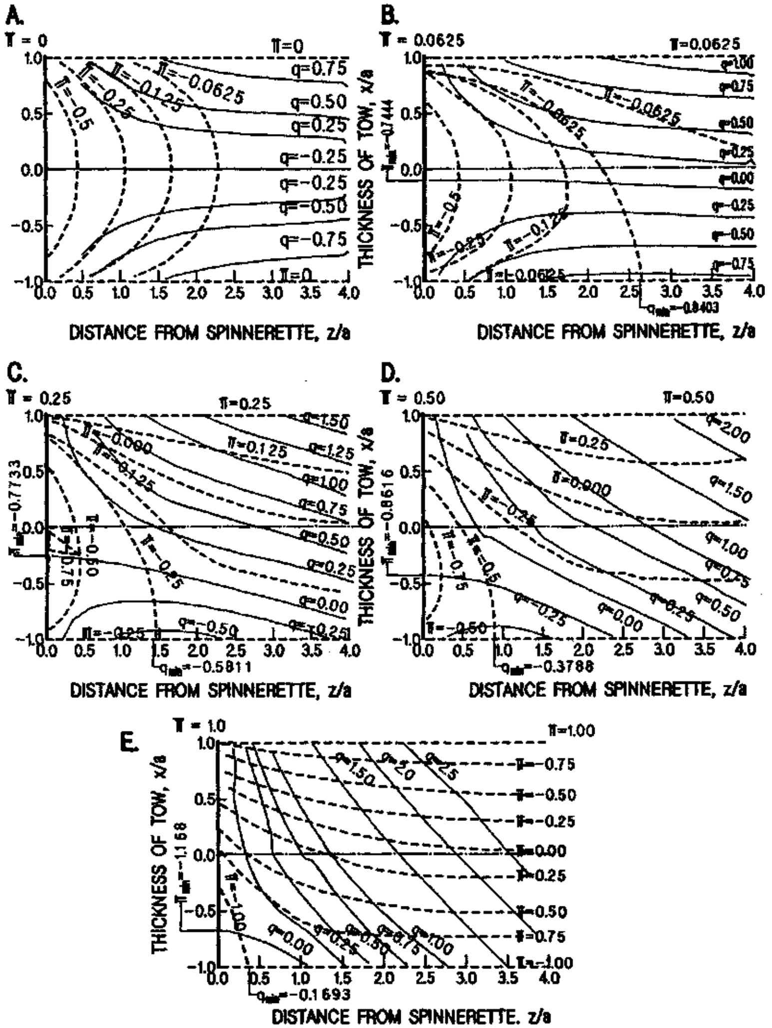

Figure VII.10: *Flat tow. Isobars, ($\tilde{\Pi}$ = const.), dashed lines, and streamlines (q = const.) full drawn lines at different values of pressure differential $\tilde{\Pi}$. After A. Szaniawski and A. Zachara.*[31]

Thus, a certain balance and compromise must be established between all of the advantages and disadvantages of high temperature extrusion.

Quite naturally, temperature of the coagulation bath cannot deviate much from the extrusion temperature, and since lacing up of the fiber tow is, more or less, a hand operation, it may be difficult to hold the bath temperature higher than what is possible for hand immersion and gloved manipulation (up to 60°C).[14]

Both for the environment's and economy's sake, the solvent used in the formation must be regenerated. The same is true for the nonsolvent if it happens to be other than water. If it is water, it must be purified prior to discharge back into environment. The expenses connected with the recovery are often held against the

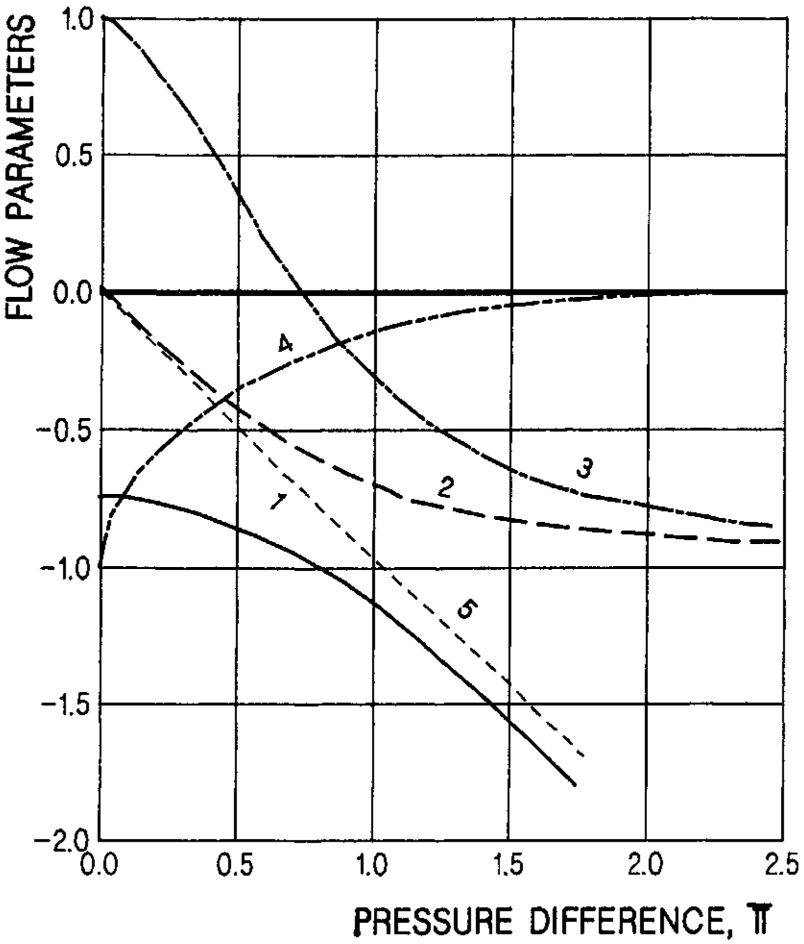

Figure VII.11: *Influence of the pressure differential on two sides of a flat tow on flow parameters. 1.* $\tilde{\Pi}_{min.} = \tilde{\Pi}(\xi_0, 0)$, *2.* $\xi_2, \tilde{\Pi}(\xi_2, 0) = \tilde{\Pi}_{min.}$; *3.* $\xi_1, \tilde{\Pi}(\xi_1, 0) = \tilde{\Pi}_{min.}$; *4.* $q_{min.} = q(-1, \xi_1)$; *5.* $-\tilde{\Pi}$. *After A. Szaniawski and A. Zachara.*[31]

viability of wet formation. In reality this notion may be or may be not true; it depends on the compounds.

If water is the nonsolvent and if the boiling point of the solvent is higher than water then water must be distilled off. This is energetically expensive, as water has a very high heat of evaporation. If the solvent is more volatile than water then the distillation expenses may be reasonable, and the rest depends on the expenses of water purification. The bulk of recovery is concentrated around distillations. Adsorption methods may be necessary to a small extent for the purification of the plant atmosphere.

Different approaches are necessary in the majority of processes involving chemical reactions during formation. Recovery of the solvent and chemicals must be treated on a case by case basis, as required by the chemistry involved.

VII.4 Dry Formation

Dry formation of fiber resembles formation from the melt much more than the wet formation does. The concentration of solutions (dopes) used ranges from some three per cent to a gel or plasticized melt. The processes involving the highest concentrations are referred to as gel spinning or plasticized melt spinning rather than a formation from solution. In the case of gel spinning, the molecular mass is usually very high ($M \geq 1000000$), so in such cases the dope concentrations are not necessarily exceedingly high; they may be within some forty to sixty percent range, or even less.[25–27]

The concentration of spinning solution is, as always, an issue of the process economy. In the technical sense, however, the fiber properties obtained from dopes of higher concentration are better.[2] Better fiber properties are also obtained from a polymer of higher molecular mass, which leads to a higher solution viscosity too. It has been found[41] that tenacity of fibers decreases if the extrusion is conducted above the point of fracture, which in some cases may occur at relatively low shear rates, occasionally as low as $100s^{-1}$; an increase of temperature does not always help. This is a good reason to keep the concentration low. The same authors[41] claim that at substantially higher shear rates fracturing may cease and fiber tenacity goes up again. Similar effects have been found also in the case of melts of block copolymers.[42] Nevertheless, there is also a voice claiming that extrusion with fracturing may lead to higher fiber tenacities, provided that the fibers are extensively drawn at high temperature.[46]

There is no doubt that in some cases the low concentration of dopes used is a matter of tradition, and in dry formation the tradition is quite old, reaching the time when the knowledge of physical chemistry of solutions and their rheology was much more limited than it is today. On other occasions, it may be a compromise between the most convenient solvent, viscosity of solution, and feasible temperature of extrusion.

All of the polymers currently processed from solution, except for the high performance polymers, have low thermal resistance, and this is the main reason for solution processing. In dry formation, contrary to the wet processes, the extruded filament enters into the air atmosphere, which may aggravate the tendency to decomposition. Even if the drying process is carried out in the atmosphere of an inert gas, it is rather difficult to keep the air completely out if the cost of equipment is not to be excessively high.

Mixed solvents may be considered and their application in dry processes may be easier than in wet ones. Again, tradition seems to be responsible for the fact that we do not see them applied yet. Improper differences in the rate of evaporation of the various components of the mixture may have some adverse effects on the resulting fiber properties or on their appearance, e.g. matted surface, etc.

Formation of fibers from solutions undergoing phase separation may be considered as a border case with formation from the melt. According to Zwick[43], solutions of three to twenty percent concentration may be spinnable at velocities of 100 to $1000m/min$. The polymer-solvent system must be chosen so that after leaving the spinnerette, the solution undergoes a phase separation into a pure polymer or its highly concentrated gel and a pure solvent phase. The expelled solvent may be dried or eventually washed away before the fiber reaches the take-up device. Solvents useful for such a method of formation must satisfy one of the following conditions:

- The temperature of extrusion must be closely above the theta- temperature, but the temperature in the drying cell is lower than theta-temperature.
- The polymer is soluble only in the liquid solvent but the solvent solidifies at temperatures a little below the temperature of extrusion.
- The solvent consists of more than one component, while none of the components alone is able to dissolve the polymer. At the same time either miscibility of the solvent components must be highly temperature dependent or one component is highly volatile and evaporates quickly after leaving the spinnerette.

Preparation of solutions for dry formation is usually carried out in conventional equipment used for the purpose in polymer processing. Dissolution of polymers is slow, often it takes around three hours. Consequently it is performed in batches, with several groups of equipment in parallel put in-line with the entire operation. Additionally, the phenomena of *aging* or *ripening* of polymer solutions need to be taken into account. Depending on the polymer-solvent system in question, on concentration, and on temperature used, it may be good to subject the solution to a longer *ripening*, but a really long storage may be difficult to incorporate into a continuous, in- line operation. When concentrated solutions are used, continuous dissolution and transport may be easier to achieve, *e.g.* by coupling a mixer and screw extruder in line.[44]

The polymer solution for dry formation must be filtered. Commonly, there are two stages of filtration. The first stage is placed immediately after dissolution to remove accidental mechanical impurities and particles of undissolved polymer (gel), etc.; the second stage filter is located just before the solution enters the spinnerette, as in melt formation. The filtering assemblies are similar to the one used for melt processes. The first stage is solely for the purification of the solution, the second stage serves mainly for the rheological and morphological purposes.

The spinnerettes for dry formation are designed according to the same principles as for the other processes. Naturally, the lower viscosity in many cases requires thinner plates due to lower extrusion pressures. The lower viscosity of solutions allows for the formation of very fine fibers, without applying excessively large extrusion pressures. After drying, the filaments become even thinner due to the loss of solvent.

Extrusion is commonly carried in a downwards configuration into a vertical drying chamber (*cell*). Upwards extrusion is used only occasionally due to a potential of dripping of low viscosity solutions. Similar problems may be associated with large diameter of filaments.

As a drying medium, the most often used is air, in rare cases an inert gas. The equipment for drying the fibers is similar to an air quench with a counter-current air flow, except that the air (or other gas) containing solvent vapors must be carefully and quantitatively withdrawn and led to the solvent recovery system. The air stream in formation from the melt serves only for cooling and is, if not blown across the fiber bundle, usually led co-currently with the filaments. In dry formation, the air is primarily a drying medium. In some processes, the solution is also cooled, but the heat balance between the solution cooling and supplying the necessary heat of evaporation usually leads to the need of heated air. According to the material and heat balance, the air is blown either in co- or counter-current.[2] There are processes known with a combination of co- and counter-current air flow.[45] In such "mixed" flow cases, the portion of filaments close to the spinnerette receives counter-current flow, while the filament portion close to the receiving is in co-current configuration. The mixed configuration requires that there is one point of air injection point and two points of air withdrawal. Depending on the heat balance, the walls of the drying chamber may need to be heated, though in all cases the wall temperature should be carefully controlled.

The volume of air and its temperature must be chosen so as to assure the fullest possible removal of the solvent. The evaporation of solvent may not be permitted to proceed too rapidly for the sake of fiber structure. Concentration of the solvent vapors in the withdrawn air must be kept below explosivity limits, which often amounts to less than 2 or 3% by volume.[2] The aerodynamic drag forces acting on filaments are also to be carefully observed; the rules are here the same as in the formation from melt.

The profile of filament temperature during drying changes in a characteristic pattern, which is similar in most of the dry processes. Shortly after leaving the spinnerette, the filament temperature drops, and this drop may be large. This is a consequence of rapid solvent evaporation. The temperature drop takes place despite the fact that the temperature of the drying air is at this point usually substantially higher than the extrusion temperature. The magnitude of the temperature drop is, as signaled earlier, related to the magnitude of heat of evaporation of the solvent used, of the local heating intensity, and of the resulting rate of evaporation. In the subsequent segments of the drying cell, the temperature of filaments rises and the changes take place at a more moderate rates. The temperature of the filaments should not be allowed to drop too low, as water from the air may condense, or even freeze. Entirely water-free air is difficult and expensive to maintain in the process.

A rapid loss of solvent takes place primarily on the fiber surface, which may cause an increase in the skin-core effect in the fiber structure, and this effect is rarely wanted, though in some cases it may be considered a "special effect". For this reason, the drying process should be carried out possibly gently. To provide for gentle drying conditions, the filaments are given a long drying time by being provided long drying chimneys (cells), on the order of three to six meters. The take-up velocities generally range between $100m/min$ and $900m/min$.[2,24]

The spin stretch in dry formation is normally very low, only of the order of two to four times. The low strength of the extruded polymer solution rarely permits higher extensions. Higher fiber velocities cause the obtaining of a higher stretch to be more difficult.

There were not many attempts to solve the problems of dry formation theoretically, at least not many appeared in publications. One of the earlier attempts was by R. G. Griskey and S. Y. Fok.[48–50] These authors attempted to calculate the changes of the solvent contents during a dry formation starting with the equation

$$\frac{\partial^2 c}{\partial \phi^2} + \frac{1}{\phi}\frac{\partial c}{\partial \phi} - \frac{Q}{\pi D \rho}\frac{\partial c_z}{\partial z} \qquad \text{(VII.79)}$$

with the designations: c is concentration of solvent in the radial direction, c_z is concentration of solvent along the fiber axis (z), ϕ is the nondimensional radial position r/R, with R being the filament radius at any given z, Q is volumetric solution flow rate, $Q = R^2 v_z \pi \rho$, v_z is velocity component in the z direction; velocity components in the radial v_r, and angular, v_θ, directions are assumed equal zero; D is diffusivity, and ρ is density of the solution.

As boundary conditions were taken: at $z = 0$ $c = c_0$ at all r; c is finite at all $r = 0$ and all z; $c_z = f(z)$ at $z = z$ and $r = R$.

Equation VII.77 can be solved only numerically. For the solution Griskey and Fok used the Gregory-Newton formula[51]

$$\begin{aligned} (c_z)^n_{m+1}\left[\frac{1}{(\Delta\phi)^2} + \frac{1}{m(\Delta\phi)^2}\right] \quad &+ \quad (c_z)^n_m\left[-\frac{2}{\Delta\phi} - \frac{1}{m(\Delta\phi)^2} + \frac{Q}{\pi\rho D\Delta z}\right] + \\ +(c_z)^n_{m-1}\left[\frac{1}{(\Delta\phi)^2}\right] \quad &- \quad (c_z)^{n+1}_m\left[\frac{1}{\Delta Z}\frac{Q}{\pi\rho D}\right] = 0 \end{aligned} \qquad \text{(VII.80)}$$

where $(c_z)^n_m = c_z(\phi_0 = m\phi, z_0 + nz)$ is concentration of the solvent at the n^{th} position along z-axis and m^{th} position along the radius. The flow rate Q was determined experimentally as a function of z alongside of the average concentrations. The diffusivity was takes as constant. At $z = 0$, the concentrations inside of the filament are known and equal, however, the concentrations at the two points outside the filament need to be known too. The authors computed them from equation VII.79 and from the following equation.

$$(c_c)^n_0\left[\frac{q}{\pi\rho\Delta z} - \frac{4}{(\Delta\phi)^2}\right] + \frac{4}{(\Delta\Phi)^2}\cdot(c_z)^n_1 - \frac{Q}{\pi\rho D\Delta z}\cdot(c_z)^{n+1}_0 = 0 \qquad \text{(VII.81)}$$

Equation VII.81 holds at $\phi = 0$, it is $m = 0$ and $\partial c/\partial r = 0$ and gives only (c_z) at $m + 1$ position. The value of the concentration at position $m + 2$ was calculated from the average concentration using Simpson's rule.

The results, experimental average and the concentrations calculated for $R/2$, by Griskey and Fok are reproduced in figure VII.12.

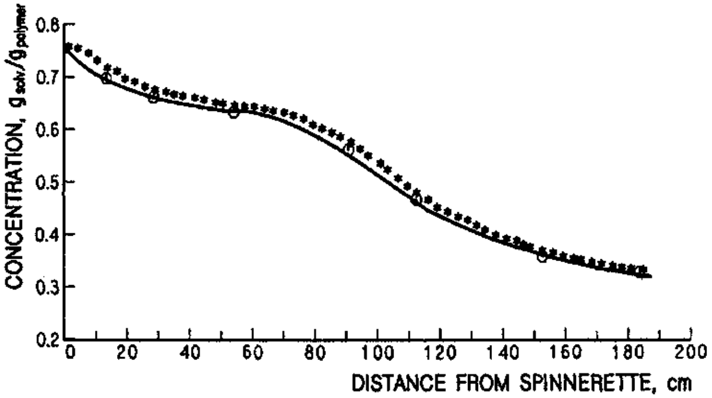

Figure VII.12: *Concentration of solvent in polymer during a dry fiber formation from poly(methyl methacrylate) in benzene. Line and circles give the experimental data average per radius, star points give the results calculated for the half of the radius. After Fok and Griskey*[49]

The experimental line presented in figure VII.12 goes though a *quasi* plateau after the initial rapid drop of solvent concentration and before a second rapid concentration decrease. Such behavior is rather usual in commercial dry formation operations and does not have any plausible explanation as of yet. The agreement between the calculated and empirical results is relatively good, and it is likely that the results might be substantially improved by more dense calculation, more points along the radius and more points along the fiber axis. It needs to be taken into account that the data for half radius do not represent the average.

A somewhat more refined solution is offered by Barzinsky and co- workers.[52] These authors consider a set of five equations. The first of these equations represents the diffusion of a solvent in the filament.

$$v\frac{\partial c}{\partial z} = D\left(\frac{1}{r}\frac{\partial c}{\partial r} + \frac{\partial^2 c}{\partial r^2}\right) + \left(\frac{\partial c}{\partial r} \times \frac{\partial D}{\partial r}\right) \qquad \text{(VII.82)}$$

Here v stands for axial filament velocity, c stands for solvent concentration in the filament, z is position along the filament axis in relation to the maximum in the die swell, r is position along the fiber radius, and D stands for diffusivity. It is worth stressing that this solution considers changes of diffusivity.

The differential energy balance is described as

$$\rho C_p v\frac{\partial T}{\partial z} = \lambda\left(\frac{1}{r}\frac{\partial T}{\partial r} + \frac{\partial^2}{\partial r^2}\right) + \left(\frac{\partial T}{\partial r} \times \frac{\partial \lambda}{\partial r}\right) \qquad \text{(VII.83)}$$

where ρ is density of the filament, T is temperature in the filament, λ is thermal conductivity, and C_p represents specific heat. The second bracketed term in equation VII.83 describes the variation of thermal conductivity.

The total material balance is given as

$$\frac{dQ}{dz} = 2\pi R M_s \alpha_m (c^* - c_a) \qquad \text{(VII.84)}$$

and the symbols here mean: Q is flow rate, R is filament radius, M_s is molecular mass of solvent, α_m is coefficient of mass transfer between the filament interface and air, c^* is the concentration of solvent in the vapor phase and in equilibrium with the liquid at the filament interface, and c_a describes the solvent concentration in the air.

The filament momentum balance is represented by

$$dF = d(\rho A v^2) + F_D dz - F_g dz - dF_{surf} \qquad \text{(VII.85)}$$

where F is tension acting on the fiber, F_D is aerodynamic drag force, F_g is force of gravity, F_{surf} is surface tension force, A is the cross sectional area of the filament, and $\rho A v^2$ represents the rate of transport of momentum.

The constitutive equation was taken to be the same as for a Newtonian fluid

$$\sigma = \zeta_T \frac{dv}{dz} \qquad \text{(VII.86)}$$

with the designation of σ as stress, and ζ_T as elongational viscosity. From equation VII.86 results that

$$F = \bar{\eta}_z A \frac{dv}{dz} \qquad \text{(VII.87)}$$

where $\bar{\eta}_T$ represents the integrated average elongational viscosity across the filament.

The boundary conditions are taken as:

- At $z = 0$ the values of r, c, T, and Q are assumed as equal to the values of the solution being extruded.
- At the take up point, the filament velocity is assumed to be equal to the circumferential velocity of the roller.
- At $r = 0$, and all z is assumed axisymmetric nature and circular cross section of the filament what means that $\partial c/\partial r = \partial T/\partial r = 0$.
- At $r = R$ at any z: $-\rho D\partial c/\partial r = \alpha_m M_s(c^* - c_a)$, and $-\alpha\partial T/\partial r = \alpha(T_s - T_a) + HM_s\alpha_m(c^* - c_a)$; and α is the heat transfer coefficient between the filament interface and the surrounding gas, H is the enthalpy of solvent evaporation, and α_m is mass transfer coefficient.

The set of equations needs to be solved numerically. Tension at the take-up point can rarely be measured, and thus may need to be assumed. Calculations according to this system show that the most dramatic changes in the process take place during the first ten millimeters from the spinnerette face. This applies to filament radius, temperature, and velocity. The filament velocity becomes constant (plug flow), while the diameter changes only due to the solvent losses taking place. The drastic changes taking place during the first instant after leaving the spinnerette are attributed to the rapid increase of viscosity due to quick solvent evaporation and the accompanying temperature drop.

The confrontation of the calculated values with the experimental data has been moderately successful. Filament radius decreased even more abruptly than predicted. Incidentally, a similar deviation is seen in the calculations by Griskey and Fok. Velocity, naturally, changes in line with the diameter changes. The deviations of the theory from the experimental data seem to be smaller here than in the corresponding theoretical solutions for fiber formation from the melt published thus far. One may speculate that the smaller deviations result from the lower viscosities and consequently smaller discrepancies between the use of the constitutional rheology equation rather than creep, which gives substantially better results for formation from the melt.

It may be important to mention that there is an analogy between the heat transfer coefficient, α, and the mass transfer coefficient in diffusion, α_m.[53] Based on this analogy, it is possible to calculate the mass transfer coefficient, α_m, from the heat transfer coefficient, which may be easier to determine.[54,55] An apparatus for the measurements has been described by T. Mitzushina and M. Nakajima.[54]

$$\ln\left(1+\frac{c_{s,0}-c_{s,\infty}}{1-c_{s,0}}\right)=\frac{\alpha}{\alpha_m C_{ps}}\left[1+\frac{\xi C_{ps}(T_\infty-T_0)}{H_{sT}}\right] \qquad \text{(VII.88)}$$

where $c_{s,0}$ and $c_{s,\infty}$ are the mole fractions of the solvent in the air before and after the solvent contact, respectively; α is heat transfer coefficient; α_m is mass transfer coefficient; T_∞ and T_0 are wet bulb and dry bulb temperature, respectively, C_{ps} is heat capacity of the solvent vapor; H_{sT} is heat of evaporation of the solvent at the dry bulb temperature; ξ is a correction coefficient which depends on the apparatus used and usually amounts to little more than one.[54]

The heat transfer coefficient may be calculated from the equations developed by Ohzawa and Nagano.[56] For the heat transfer related to a situation where the entrained convection is superimposed on the forced parallel convection, the proposed equation is

$$\alpha=\frac{0.886\lambda^*}{\sqrt{A}}\left[0.35+0.146\left(\frac{1.129\sqrt{A}U_p}{\nu}+R\right)^{0.5}\right] \qquad \text{(VII.89)}$$

where

$$R=\left[1.076\left(\frac{\sqrt{A}v_z}{\nu}\right)^{0.36}-0.685\right]^2 \qquad (VII.89\,a)$$

where α is heat transfer coefficient, λ^* is heat conductivity at the interface, A is filament cross section area, U_p is the velocity of forced air (gas) parallel to the filament, ν is kinematic viscosity in the interface, v_z filament velocity in the axial direction.

For the case of the entrained convection and superimposed perpendicular convection the equation is

$$\alpha=\frac{0.886\lambda^*}{\sqrt{A}}\left[0.35+0.50\left(\frac{1.129\sqrt{A}U_c}{\nu}+R\right)^{0.5}\right] \qquad \text{(VII.90)}$$

where

$$R = \left[0.313\left(\frac{\sqrt{A}v_z}{\nu}\right)^{0.36} - 0.20\right]^2 \qquad (VII.90\,a)$$

Here U_c means air velocity in cross flow.*

The spun fibers in the dry processes are mostly highly crystalline and of low crystalline orientation.[2] Normally, it is difficult to remove the solvent completely from the spun fibers. When fibers are subjected to a neck drawing, it is performed in a separate operation. For this reason, a substantial secondary crystallization, enhanced by the presence of the residual solvent, takes place after the extrusion and drying and before drawing. These processes depend, naturally, on the crystallization propensity of the polymer in question; on the other hand, there are few polymers which crystallize poorly in the presence of solvent, if they crystallize at all.

When fibers have a strong skin-core structure, which may be considered as a structural inhomogeneity, highly inhomogeneous drawn fibers, with a large volume of cracks and voids may be formed. If there is any stronger orientation in spun fibers, then most probably it is limited to the skin, which has coagulated earlier and was exposed to the tension longer.[53] Such a structural inhomogeneity may cause further deepening of this effect in the subsequent drawing operation. To remove residual solvent from spun fibers, washing – extraction may be used,[2] though this is usually done when the fibers are not subjected to neck drawing operation.

The large amounts of solvents used in the dry fiber formation must be recovered to prevent pollution of the environment. Also, the solvent must be removed from the air not to create an explosion or fire hazards. At the same time the recovery is needed to enhance the process economy. The content of solvent in the drying gas is normally very low, condensation alone is normally entirely insufficient or outright inappropriate and therfore it is rarely used. To remove the solvent from gas (air), the mixture is separated through adsorption of the solvent on activated carbon, or sometimes on silica gel. It is rather expensive process, both in investment and maintenance of the carbon beds.

By subjecting the spun fibers to neck drawing, their tensile properties may be improved. However, the high degree of crystallinity present in dry formed fibers, the voids in the internal structure, as well as the non-uniformities of the fiber cross sections due to the skin roughness make it difficult to perform a drawing operation, particularly a more extensive drawing and at commercially interesting speeds. Naturally, the drawing operations, if performed, are carried out at elevated temperatures, similar to the analogous treatment of fibers formed from melt. If a high degree of porosity, is present in the solution formed fibers, the drawing operations become additionally troublesome. In very difficult cases, one may resort to swelling of the fibers just prior to, or during, neck drawing. Hot water,[54] or glycerol bath,[55,56] or water steam[57,58] may be used as the swelling medium.

---

*Data on some of the physical properties and their functions of temperature are given in the Appendix.

The liquids or vapors used must be able to swell the polymer, but any stronger dissolving power is to be avoided. The most ideal are liquids or vapors then which are not able to swell crystalline and oriented polymer structures. Preferably, they should affect only amorphous portions of the structure. In such ideal cases, a large portion of the swelling agent is expelled from the fiber structure in the necking. If the swelling agent is strong, then it must be removed immediately after drawing; otherwise the fibers would shrink back to *undo* the gains obtained in drawing.

Like in the other methods of formation, dry formed fibers may be subjected to post treatments. Sometimes a post treatment is simply necessary. The most frequently applied means are: washing and annealing. The purpose of washing is mainly to remove residues of solvents and/or processing finishes remaining in the fibers, and sometimes quite stubbornly. Annealing is used primarily for general stabilization of the fiber structure, though it may also help in removal of the unnecessary residuals. A successful structure stabilization through annealing is possible only when all solvents or swelling agents are removed from the fiber.

Heat treatment of some polymers may result in some degree of cross linking, even without the use of cross linking agents. In some fibers, a small amount of cross linking introduced into already formed fibers may have a highly beneficial influence on the fiber properties. Such fiber modifications are occasionally taken advantage of.[2]

VII.5 References

1. *Ger. Pat.* No. 38,368 (1885).
2. W. Frey and A. Sippel in *Fasern aus synthetischen Polymeren*, ed. by R. Hill, Berliner Union Verlag, Stuttgart, 1956, pp. 407 - 426.
3. P. H. Geil: *Polymer Single Crystals*, Interscience Publ., New York, 1963, pp. 86, 382.
4. D. C. Basset, A. Keller, and S. Nitsuhashi, *J. Polymer Sci.*, **A1 (1963)**, 763.
5. H. D. Keith and E. J. Padden, Jr., *J. Appl. Phys.*, **34 (1963)**, 2409.
6. H. A. Lanceley and A. Sharples, *Makromol. Chem.*, **94 (1966)**, 30.
7. L. Mandelkern: *Growth and Perfection of Crystals*, John Wiley and Sons, New York, 1958, p. 490.
8. J. G. Fatou, E. Riande, and R. Garcia Valdecasas, *J. Polymer Sci., (Phys.)*, **13 (1975)**, 2103.
9. A. B. Dessai and G. L. Wilkes, *J. Polymer Sci., Symposia*, **No. 46 (1974)**, 291.
10. R. M. Secor, *A. I. Ch. E., J.*, **11 (1965)**, 482.
11. A. T. Serkov, G. J. Kudryavcev, V. S. Klimenkov, L. A. Serkova, and Yu. P. Kozhevnikov, *Faserforsch. Textitech.*, **20 (1969)**, 125.
12. J. J. Hermans, *J. Colloid Sci.*, **2 (1947)**, 387.
13. J. R. Booth, *A. C. S. Polymer Preprints*, **7 (1966)**, 759.
14. J. M. Preston in *Fasern aus synthetischen Polymeren*, e. by R. Hill, Berline Union Verlag, Stuttgart, 1956, pp. 389 - 405.

15. V. Gröbe and R. Gieske, *Faserforsch. Textitech.*, **20 (1969)**, 30.
16. V. Gröbe and H. J. Gensrich, *Faserforsch. Textiltech.*, **20 (1969)**, 118, 425.
17. M. C. Botty, C. D. Felton, and R. E. Anderson, *Text. Res. J.*, **30 (1960)**, 959.
18. P. H. Hermans: *Physics and Chemistry of Cellulose Fibers*, Elsevier Publ., New York, 1949.
19. H. Fujita, *J. Chem. Phys.*, **21 (1953)**, 700.
20. Sin Yuen Fok and R. G. Griskey, *J. Appl. Polymer Sci.*, **11 (1967)**, 2417.
21. J. R. Griffin and D. R. Coghanowr, *A. I. Ch. E., J.*, **11 (1965)**, 133, 1521, 246.
22. A. Rende, *J. Appl. Polymer Sci.*, **16 (1972)**, 585.
23. H. Gröber, S, Erk, and V. Girgull: *Die Gruntgesetze der Wärme- übertragung*, Springer Verlag, Berlin - Göttingen - Heidelberg, 1955.
24. T. Rosner and H. Wójcikiewicz: *Włókna syntetyczne* (Synthetic Fibers), Wydawnictwo Naukowo-Techniczne, Warszawa, 1969.
25. Swiss Pat. No. 314,609.
26. Brit. Pat. No. 1,021,972.
27. U. S. Pat. No. 2,822,237.
28. D. Machin and C. E. Rogers, *Makromol. Chem.*, **155 (1972**, 269.
29. R. M. Griffith, *Ind. Eng. Chem.*, **3 (1964)**, 245.
30. A. Szaniawski and A. Zachara, *Polimery* (in Polish), **19 (1974)**, 143.
31. A. Szaniawski and A. Zachara, *Polimery* (in Polish), **20 (1975)**, 87.
32. P. J. Flory: *Principles of Polymer Chemistry*, Cornell University Press, Ithaca, 1967, p. 548 ff.
33. H. Fujita, *Fortschr. Hochpolymer. - Forsch.*, **3 (1961)**, 1.
34. R. M. Vasenin, *Vysokomol. Soyedin.*, **2 (1960)**, 851. 34
35. T. G. Fox, *Bull. Am. Phys. Soc.*, **1 (1956)**, 121.
36. F. N. Kelly and F. Bueche, *J. Polymer Sci.*, **50 (1961)**, 549.
37. E. Jenckel and R. Heusch, *Kolloid-Z.*, **13 (1953)**, 89. 37
38. G. Kanig, *Kolloid-Z.*, **190 (1963)**, 1.
39. U. S. Pat. No. 2,451,420.
40. G. A. Danilin, *Khim. Vol'okna*, **(1981)**, 22.
41. J. H. Southern and R. L. Ballman, *Text. Res. J.*, **53 (1983)**,230.
42. Z. K. Walczak, *previously unpublished results*, 1982.
43. M. M. Zwick, *A.C.S. Polymer Preprints*, **7 (1966)**, 814; *Appl. Polymer Symp.)*, **No. 6 (1967)**, 109.
44. E. Masłowski, *Polimery*, (in Polish) **9 (1966)**, 429.
45. *Netherl. Pat.* No.66,15,961.
46. S. Gogolewski, A. J. Pennings, *J. Appl. Polymer Sci.*, **28 (1983)**, 1045.
47. Ye. Alyeva, Yu. P. Kozhevnikov, V. A. Medvedev, and A. T. Serkov, *Khim. Vol'okna*, **(1990)**, 6.
48. S. Y. Fok and R. G. Griskey, *Appl. Sci. Res.*, **16 (1966)**, 141.
49. S. Y. Fok and R. G. Griskey, *J. Appl. Polymer Sci.*, **11 (1967)**, 2417.

50. R. G. Griskey and S. Y. Fok, *Fundamental Consideration of Dry Spinning*, paper presented at A. I. Ch. E. Meeting, Atlanta, February, 1970.
51. K. S. Kunz: *Numerical Analysis*, McGraw - Hill, New York, 1957, p. 275.
52. I. Barzinsky, A. G. Williams, and H. L. LaNieve, *Polymer Eng. Sci.*, **15 (1975)**, 834.
53. R. B. Bird, W. E. Stewart, and E. N. Lightfoot: *Transport Phenomena*, John Wiley and Sons, New York, 1960, p. 667.
54. T. Mitzushina and M. Nakajima, *Kagaku Kikai*, **15 (1951)**, 30.
55. Y. Ohzawa, Y. Nagano, and Y. Matsuo, *J. Appl. Polymer Sci.*, **13 (1969)**, 257.
56. Y. Ohzawa, and Y. Nagano, *J. Appl. Polymer Sci.*, **14 (1970)**, 1879.
57. V. Elsasser, *Kolloid-Z.*, **113 (1949)**, 37.
58. *French Pat.* No. 913,927.
59. H. Rein, *Angew. Chem.*, **60A (1948)**, 159.
60. P. A. Koch, *Textil Rundschau*, **5 (1950)**, 414.
61. *U. S. Pat.*, No. 2,418,507.
62. *U. S. Pat.*, No. 2,420,565.
63. F. Fushimi, T. Watanabe, T. Hiyoshi, Y. Yamashita, and T. Osakai, *J. Appl. Polymer Sci.*, **59 (1996)**, 15.